Distributed formation control for port-Hamiltonian multi-agent systems by average state estimation⋆

Jingyi Zhao[a], Yongxin Wu[b,*], Yuqian Guo[c], Li Zhu[a], Yuhu Wu[a]

[a]*The Key Laboratory of Intelligent Control and Optimization for Industrial Equipment of Ministry of Education and the School of Control Science and Engineering, Dalian University of Technology, Dalian, 116024, China*
[b] *Université Marie et Louis Pasteur, SUPMICROTECH, CNRS, institut FEMTO-ST, F-25000 Besançon, France*
[c]*The School of Automation, Central South University, Changsha, 410083, China*

Abstract

In recent years, propelled by the rapid development of information technology and the Internet, the formation control of multi-agent systems has gradually emerged as a research hotspot. This paper focuses on the formation control problem of multi-agent mechanical systems with port-Hamiltonian (PH) dynamics. Firstly, the formation problem is converted to an optimization problem whose solution meets the formation requirements. Subsequently, in order to guide the closed-loop system to converge to the solution of this optimization problem, we propose two distributed controllers. The first controller is designed for multi-agent systems where the formation output is defined by position. Notably, this controller preserves the PH structure in the closed-loop, which simplifies the selection of candidate Lyapunov functions for proving the asymptotic convergence of the system to the desired formation. To characterize the minimum convergence rate of the closed-loop system, the second controller is proposed. Based on this controller, the exponential stability and the minimum convergence rate of the closed-loop system are provided. Additionally, these controllers only require agents to exchange estimations of the average state with their neighbors, thereby protecting the privacy of their state and value function information. Finally, the effectiveness of these controllers is verified through an application case on nonholonomic wheeled robots.

Keywords: formation control, port-Hamiltonian systems, distributed controller, state protection.

1. Introduction

Due to the practical potential in various applications and the theoretical challenges of collaborative control in multi-agent systems, significant research efforts have been devoted to this field [1]. Formation control, as one of the most active research topics in collaborative control, generally aims to satisfy prescribed constraints on states of multi-agent systems based on local and partial information [2]. Consequently, distributed controllers, which require only local information, have broader applications in formation control problems and can reduce the burden of network communication compared to centralized controllers that require global information [3].

At present, there have been numerous achievements in formation control, such as in [4, 5, 6, 7, 8]. Focusing on the formation control of a fleet of unmanned surface vehicles, Zhang et al. [9] proposed a distributed global output-feedback control scheme to achieve the formation control without velocity measurement. The results of a study on nonlinear symmetric control systems in [10] contribute to the stability of a large-scale system interconnected by a given number of components. These findings can also be applied to the shape formation of multiple robots. Based on aggregative games, Deng et al. designed different distributed algorithms for multiple quadrotor unmanned aerial vehicles [11] and high-order multi-agent systems [12]. Further details can be found in [13].

⋆This work was supported by China Natural Science Foundation (No.62173062 and No.$U24A20263$), and the EIPHI Graduate School (contract ANR-17-EURE-0002).

*Corresponding author. E-mail address: yongxin.wu@femto-st.fr

Recently, the port-Hamiltonian (PH) system has often been chosen to describe the agent's dynamics by emphasizing its physical properties and interconnection characteristics. Under the PH framework, the agents are interconnected using a well-defined geometric structure and the interconnected ports [14]. The PH structure has proven to be particularly suitable for control design due to its passivity [14, 15]. A wide range of complex systems in multi-physical domains could be described by PH dynamics, including the important class of mechanical systems and several chemical, electromechanical, and electrical systems. For example, Matei et al. [16] modeled the interacting particle systems by virtue of the PH framework and analyzed their dynamical properties. In addition, Donaire et al. [17] mentioned that some systems allow Hamiltonian but not Lagrangian representations, and in [18], the PH framework is more convenient and natural in spacecraft dynamics than the Lagrangian.

There are some related results regarding the control of PH systems. For example, Kumar et al. [19] investigated the tracking control for the fractional order system with PH dynamics and designed an effective controller. However, this work is only useful for the control of single and chaotic fractional order systems. For the formation or tracking control in multi-agent systems in the PH framework, some researchers have made efforts. For example, Vos et al. [20] presented a controller for a fleet of nonholonomic wheeled robots to accomplish the formation as well as velocity tracking control. Subsequently, they investigated a specific formation control problem of multiple agents with coulomb friction in [21]. Javanmardi et al. [18] used the leader-multi-followers architecture to develop tracking controllers for spacecraft formation flying based on Interconnection Damping Assignment Passivity-Based Control (IDA-PBC). Notably, these works are primarily based on traditional methods, such as energy shaping, damping injection, and IDA-PBC, and aim at a specific mechanical system dynamic or a specific formation control problem like leader-follower formation. Li et al. [22, 23] proposed an approach for many different types of formation control problems of mechanical systems. However, in this work, every agent directly exchanges states with their neighbors, which may cause privacy concerns.

In many practical situations, sensitive information leakage generally has negative effects on the normal operation of the multi-agent systems, even disrupting or devastating it, as described in [24]. For example, Yue et al. [25] mentioned that cooperative formation is a typical swarm behavior by which multiple Unmanned Aerial Vehicles (UAVs) execute combat missions, and recently research has focused on the privacy-preserving issues in the process of multiple UAVs' cooperative formation control. Specifically, in typical applications where UAVs from different stakeholders conduct joint operations, and the formed UAV swarm is used as monitoring units, each USV carries sensitive information from its group, hence, the protection of its individual privacy is particularly significant. Considering the protection requirements of sensitive information in the formation control of multi-agent systems, some researchers have proposed control schemes, like homomorphic encryption [26], differential privacy [27]. These methods effectively protect agents' privacy information using encryption, decryption, or perturbations. However, encrypting and decrypting messages are complex and cause time delays. To the best of the authors' knowledge, no research has been conducted on the formation control problems for multiple PH systems with privacy protection. This gap motivates us to explore the distributed formation controller with privacy protection within the PH framework.

Different from these works as [11, 12, 28, 29], we consider multiple mechanical systems with PH dynamics, due to the PH framework's inherent advantage in its physical systems' descriptive capability, property of interconnection, and extensive applicability. Firstly, a distributed controller is proposed when the formation output is equal to the position. Under the action of this controller, the overall multi-agent closed-loop system maintains the PH structure and is asymptotically stable. The PH structure admits the *Hamiltonian* function to be chosen as a candidate Lyapunov function, which decreases the difficulty of stability analysis. To furnish a well-defined quantitative metric for the convergence rate of the system, the second controller is designed, based on which, the exponential stability of the corresponding closed-loop system is proved in theory, although the design of the formation output function disrupts its PH structure. Meanwhile, these two distributed controllers do not require the agents to obtain the state of their neighbours and, therefore, protect agents' privacy. The main contributions are listed as follows.

(1) Different from [21, 30, 31, 32], under the proposed controllers, the agents exchange information through the average state estimations and the error auxiliary variables instead of the exact states with their neighbors. This approach protects agents' state and value function, while achieving the desired formation.

(2) The first controller preserves the PH structure of the multi-agent systems, with the *Hamiltonian* naturally serving as a Lyapunov function candidate. This simplifies the selection of a Lyapunov function for stability analysis compared to the previous studies in [11, 12, 31, 33].

(3) Inspired by the first controller and those proposed in previous works [20, 34, 35], the controllers in these works

guarantee asymptotic stability, where the convergence rate cannot be estimated. In contrast, the second proposed controller is designed to ensure the exponential stability of the desired formation. It can achieve a convergence rate greater than a specified value, thus theoretically offering a convergence guarantee with a minimum convergence rate.

The remainder is organized as follows. Section 2 provides essential preliminaries, then, Section 3 describes the considered formation control problem. Section 4 proposes two controllers and analyzes the stability of the corresponding closed-loop systems, respectively. Section 5 presents a simulation example, and the final section concludes the work and gives some perspectives.

2. Preliminaries

In this section, the notations and preliminaries mainly used in this work are introduced.

2.1. Notations

The symbol $\mathbb{R}^n$ denotes the n-dimensional Euclidean space and $\mathbb{Z}$ denotes the set of integers. $1_n \in \mathbb{R}^n$ and $0_n \in \mathbb{R}^n$ represent the vectors with all components being one and zero, respectively. $\|\cdot\|$ denotes the Euclidean norm. The Kronecker product is denoted by $\otimes$. $A = (a_{ij})_{N\times N}$ denotes the matrix $A \in \mathbb{R}^{N\times N}$ with the element in row i and column j being $a_{ij} \in \mathbb{R}$. $\|x\|_A^2 := x^\top Ax$ is the norm of the vector $x \in \mathbb{R}^m$ with respect to the matrix $A \in \mathbb{R}^{m\times m}$, where $x^\top$ is the transpose of x. For an invertible matrix A, the symbol $A^{-\top}$ is short for $(A^{-1})^\top$. For any two integers $i, j \in \mathbb{Z}$ with $0 < i < j$, $[i : j]$ dentoes the set of successive integers $\{i, i+1, \cdots, j-1, j\}$. For a collection of columns vectors $x_i \in \mathbb{R}^m$, $i \in [1{:}N]$, $\mathrm{col}(x_1, \cdots, x_N) := (x_1^\top, \cdots, x_N^\top)^\top \in \mathbb{R}^{Nm}$. For a collection of diagonal matrices $Q_i \in \mathbb{R}^{m\times m}$, $i \in [1{:}N]$, and any $j \in [1{:}m]$, Q_{ij} represents the jth diagonal element of Q_i. I_n is an identity matrix in $\mathbb{R}^{n\times n}$. $\mathrm{diag}(\lambda_1, \cdots, \lambda_n) \in \mathbb{R}^{n\times n}$ is the diagonal matrix of elements $\lambda_1, \cdots, \lambda_n \in \mathbb{R}$. For any ordered index set $\mathcal{S} = [1{:}s]$, $\eta_\mathcal{S}$ is short for the vector $(\eta_1, \cdots, \eta_s)$.

2.2. Some basic concepts

This paper considers N agents communicating over an undirected connected graph $\mathcal{G} := \{\mathcal{V}, \mathcal{E}, \mathcal{A}\}$, where $\mathcal{V} = [1{:}N]$ represents the node set, $\mathcal{E} \subseteq \mathcal{V}\times\mathcal{V}$ represents the edge set, and the symmetric matrix $\mathcal{A} := (a_{ij})_{N\times N}$ represents the adjacency matrix. The agent $i \in \mathcal{V}$ is a neighbour of $j \in \mathcal{V}$ if $(i, j) \in \mathcal{E}$, in which case $a_{ij} = 1$. Otherwise, if $(i, j) \notin \mathcal{E}$, then $a_{ij} = 0$. That is, if i is a neighbour of j, then j is also a neighbour of i. Moreover, we always assume that for any $i \in \mathcal{V}$, it holds that $a_{ii} = 0$. The set of all neighbours of i is denoted by $\mathcal{N}(i) := \{j \in \mathcal{V} | a_{ij} = 1\}$. The degree matrix is defined as $\mathcal{D} := \mathrm{diag}(\deg_1, \cdots, \deg_N)$, where $\deg_i := \sum_{j=1}^N a_{ij}$, $i \in [1{:}N]$, and the Laplacian matrix of $\mathcal{G}$ is defined by $L := \mathcal{D} - \mathcal{A}$. The eigenvalues of L are denoted by $\lambda_1 \le \cdots \le \lambda_N$. If there exists a connection path from any node to another, $\mathcal{G}$ is said to be connected. A criterion is that $\mathcal{G}$ is connected if and only if $\lambda_2 > 0$. To find more details, please see [36].

In addition to the above-mentioned graph-related concepts, some important properties and definitions of functions are also involved in this paper. A function $f : \mathbb{R}^n \to \mathbb{R}^n$ is L_f-Lipschitz ($L_f > 0$) on $\mathbb{R}^n$ if $\|f(x) - f(x')\| \le L_f\|x - x'\|$ is satisfied for all $x, x' \in \mathbb{R}^n$. If there exists a $w > 0$ such that $(x - x')^\top(f(x) - f(x')) \ge w\|x - x'\|^2$ holds for all $x, x' \in \mathbb{R}^n$, the function $f : \mathbb{R}^n \to \mathbb{R}^n$ is w-strongly monotone. More details about the above definitions can be found in [37].

2.3. The PH model of mechanical agents

The ith ($i \in \mathcal{V}$) agent's dynamic is described by the following standard PH system[1] :

$$\begin{cases} \dot{x}_i = (J_i(x_i) - R_i(x_i))\frac{\partial H_i(x_i)}{\partial x_i} + g_i(x_i)u_i, \\ y_i = g_i^T(x_i)\frac{\partial H_i(x_i)}{\partial x_i}, \end{cases} \tag{1}$$

where $x_i \in \mathbb{R}^{\tilde{m}}$ represents the state of the ith agent, the smooth function $H_i(x_i) : \mathbb{R}^{\tilde{m}} \to \mathbb{R}$ represents the total energy of the ith agent called the *Hamiltonian* function, the structure matrix $J_i(x_i) : \mathbb{R}^{\tilde{m}} \to \mathbb{R}^{\tilde{m}\times\tilde{m}}$ satisfies $J_i(x_i) = -J_i^\top(x_i)$,

[1] In system (1), $x_i = x_i(t), u_i = u_i(t), J_i(x_i) = J_i(x_i(t)), R_i(x_i) = R_i(x_i(t)), H_i(x_i) = H_i(x_i(t)), g_i = g_i(x_i(t)), y_i = y_i(t)$. In the following text, for simplicity of description, t is omitted without causing ambiguity.

the dissipation matrix $R_i(x_i) : \mathbb{R}^{\tilde{m}} \to \mathbb{R}^{\tilde{m}\times\tilde{m}}$ is a symmetric semi-positive definite matrix, that is $R_i(x_i) = R_i^\top(x_i) \geq 0$. $g_i(x_i) : \mathbb{R}^{\tilde{m}} \to \mathbb{R}^{\tilde{m}\times n}$ is called the input mapping. The control input $u_i \in \mathbb{R}^n$ and the system output $y_i \in \mathbb{R}^n$ are power conjugated variables, like force and velocity in a mechanical system or current and voltage in a circuit.

In this work, we mainly focus on the formation control of multiple mobile mechanical systems such as unmanned aerial vehicles (UAVs) [38] and robots [39], which are of a natural PH structure. In system (1), let m and m_p be positive integers such that $m + m_p = \tilde{m}$. We define the state of the ith ($i \in \mathcal{V}$) agent as $x_i = \mathrm{col}(q_i, p_i)$, where the position $q_i \in \mathbb{R}^m$ and the momentum $p_i \in \mathbb{R}^{m_p}$. Then, the dynamic of the ith agent can be described as

$$\begin{cases} \dot{q}_i = A_i(q_i, p_i)\frac{\partial H_i(q_i,p_i)}{\partial q_i} + B_i(q_i, p_i)\frac{\partial H_i(q_i,p_i)}{\partial p_i}, \\ \dot{p}_i = C_i(q_i, p_i)\frac{\partial H_i(q_i,p_i)}{\partial q_i} + D_i(q_i, p_i)\frac{\partial H_i(q_i,p_i)}{\partial p_i} + \tilde{g}_i(q_i, p_i)u_i, \end{cases} \tag{2}$$

where $\tilde{g}_i(q_i, p_i) \in \mathbb{R}^{m_p\times n}$ is of full row rank. We decompose the structural matrix as

$$\begin{bmatrix} A_i(q_i, p_i) & B_i(q_i, p_i) \\ C_i(q_i, p_i) & D_i(q_i, p_i) \end{bmatrix} = J_i(q_i, p_i) - R_i(q_i, p_i),$$

and define

$$g_i(q_i, p_i) = \mathrm{col}(0_{m\times n}, \tilde{g}_i(q_i, p_i)).$$

Based on the above analysis, we have shown that the mechanical system (2) is an equivalent expression of system (1) with the *Hamiltonian* function $H_i(q_i, p_i)$.

3. The motivation example and problem formulation

This section presents the formation control problem of multi-agent systems described in the PH form, commencing with a motivating example.

3.1. Formation control of multiple wheeled robots

Consider a practical scenario. There are $N = 10$ wheeled robots with PH dynamics described by (2). These robots communicate over an undirected connected graph $\mathcal{G}$. They move from their initial positions to form a certain shape on a square to perform a cooperative task. A specific example is shown in Fig.1, where the left figure illustrates the initial positions (red points) of the 10 agents, and the right one shows the desired formation, i.e., one of the blue pentagrams.

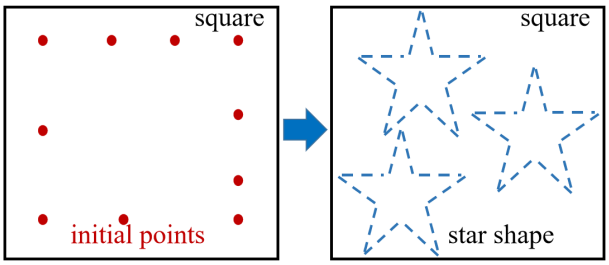

Figure 1: The diagram of a pentagram formation problem.

As in [40], the formation goal is mathematically expressed as

$$\lim_{t\to\infty} \|q_i(t) - q_j(t) - \delta_{ij}^*\| = 0, \quad i, j \in \mathcal{V}, \tag{3}$$

where $q_i(t)$ and $q_j(t)$ are the position of agent i and agent j ($i, j \in \mathcal{V}$, $t \geq 0$), respectively. In general, the constant vector δ_{ij}^* is the predefined displacement difference between agent i and agent j. The desired displacement differences between agents are determined by the desired formation satisfying

$$\delta_{ij}^* = -\delta_{ji}^*, \quad \delta_{ik}^* + \delta_{kj}^* = \delta_{ij}^*, \quad \forall i, k, j \in \mathcal{V}.$$

Remark 1. *When $\delta_{ij}^* = 0$, Eq.* (3) *becomes* $\lim_{t\to\infty} \|q_i - q_j\| = 0, i, j \in \mathcal{V}$*, and this describes a state consensus problem [41]. If the* 1*st agent is the leader, others are the followers, then the formation goal* $\lim_{t\to\infty} \|q_i - q_1 - \delta_{i1}^*\| = 0, i \in \mathcal{V}$ *describes a leader-follower formation problem [21, 28, 31, 42]. Thus, Eq.* (3) *can also describe the leader-follower formation goals.*

However, the formation objective (3) allows us to ascertain whether the desired shape has formed but not to determine its location. As illustrated in Fig.1, we cannot determine which blue pentagram is wanted. From an ornamental perspective, we hope all robots achieve the formation and perform near the center of the square (green pentagram) as Fig.2. Consequently, a simple single-objective formation problem (like in [43]) is insufficient to address this issue.

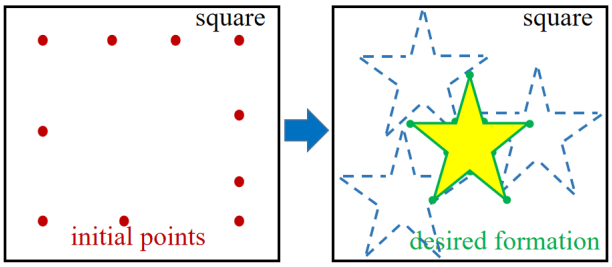

Figure 2: The diagram of a pentagram formation at the center.

Hence, to achieve the target formation in the desired location, the value function V_{1i} of the ith agent ($i \in \mathcal{V}$) is formulated as

$$V_{1i} = \frac{1}{2}\sum_{i=1}^{N} \|q_i - q_j - \delta_{ij}^*\|_{P_i}^2 + \frac{1}{2}\|q_i - \beta^*\|_{Q_i}^2, \tag{4}$$

where $P_i, Q_i \in \mathbb{R}^{m\times m}$ are symmetric positive definite matrices, β^* is the location coordinate of the center of the square. We aim to develop a controller for the ith ($i \in \mathcal{V}$) agent under the action of which, the position $q_i(0) \to q_i^*$, $t \to \infty$, where $q_i^* = \text{argmin}_{q_i\in\mathbb{R}^m} V_{1i}$ implies that the desired formation is formed.

The value function V_{1i} contains two parts:

(1) The first item of the value function V_{1i} in (4) is designed to ensure formation (3) can be achieved.

(2) The second item[2] of (4) is designed as a target position constraint.

Remark 2. *It is useful to consider the formation problem in optimization theory, such as in [33]. In practical applications of the formation control, it is reasonable to consider other requirements like destination location and fuel restrictions [44].*

Accordingly, the value function (4) of the formation objectives is comprised of the above two parts. Based on the requirements, the first objective, representing the formation goal, is of greater importance than the second one. Hence, we design the diagonal elements of Q_i, P_i satisfy $Q_{ij} << P_{ij}$, $j \in [1{:}m]$ to enlarge the weight of the first item, such that the desired formation is ensured. This approach is common in optimization problems [45].

3.2. Formation control without direct state exchange

3.2.1. Formation objective

Based on the motivation example mentioned in Section 3.1, we define the formation output function

$$\psi_i(q_i) : \mathbb{R}^m \to \mathbb{R}^l.$$

[2]This goal can also be described as an agent wanting to reach the center of the square. However, since each agent in the pentagram formation needs to be distributed at specific positions, if one agent is located at the center of the square, it will disrupt the geometric structure of the pentagram, causing the geometric center of the pentagram not to be at the center of the square. Therefore, we design this item to weigh each agent's requirement to obtain a formation close to the center of the square.

Then, the objective (4) is written in a more general form as

$$V_{2i} = \frac{1}{2}(\sum_{i=1}^{N} \|\psi_i(q_i) - \psi_j(q_j) - \delta_{ij}^*\|_{P_i}^2 + \|\psi_i(q_i) - \beta^*\|_{Q_i}^2). \tag{5}$$

If we choose $\psi_i(q_i) = \tilde{K}_i q_i$ with $\tilde{K}_i = I$, the objective (5) degenerates into (4).

3.2.2. State protection

To calculate the value function V_{1i} in (4), it is necessary for every agent to obtain its own position q_i and the position q_j of its neighbours $j \in \mathcal{N}(i)$. However, this is nearly impossible due to privacy concerns.

Remark 3. *In the aforementioned approaches of the formation control of multiple PH systems, such as those presented in [22, 30, 32], each agent explicitly discloses their states to their neighbors. However, the direct exchange of states may result in significant privacy concerns in practical applications. For instance, in the rendezvous problem, the control objective can be described as* (4) *with* $Q_i = 0_{m\times m}$ *and* $\delta_{ij}^* = 0_m$, $i, j \in \mathcal{V}$. *If agents exchange explicit states, the initial location may be revealed to neighboring agents. This situation is undesirable, as pointed out in [46].*

In the considered communication topology, each agent only is allowed to exchange information with neighbours. Consequently, without global information, a distributed algorithm rather than a centralized controller is employed to accomplish the formation objective.

Then we aim to develop a distributed controller u_i for the ith agent ($i \in \mathcal{V}$) such that under the action of the controller, the ith agent converges to the minimum point q_i^* of the optimization problem (5). To safeguard the state information of each agent, the controller u_i is designed to be only related to its own position q_i and is independent of the state of other agents.

3.3. Problem formation

To avoid disclosing private state information such as the position of each agent, we consider the average formation output $\psi_{ave}(q)$ of all agents:

$$\psi_{ave}(q) = \frac{1}{N}\sum_{i=1}^{N} \psi_i(q_i),$$

where $q = \mathrm{col}(q_1, \cdots, q_N)$. To further illustrate the physical meaning of the average formation output, we see an example first. Let $\psi_i(q_i) = q_i$, then we have $\psi_{ave}(q) = q_{ave} = \frac{1}{N}\sum_{i=1}^{N} q_i$. In this case, the average formation output q_{ave} is equivalent to the geometric center of all agents' positions, clearly demonstrating that the average formation output can be regarded as a representation of this central location.

With privacy concerns, the estimation $\hat{\eta}_i(t)$ of the ith agent ($i \in \mathcal{V}$) to the average formation output $\psi_{ave}(q)$ is designed, and we hope the estimation $\hat{\eta}_i(t)$ of the agent $i \in \mathcal{V}$ converges exactly to $\psi_{ave}(q)$ as

$$\hat{\eta}_i(t) \to \psi_{ave}(q(t)), \quad t \to \infty, \quad i \in \mathcal{V},$$

the rigorous mathematical analysis will be given in Section 4.

Define $\delta_i(t)$ as the displacement deviation between the formation output $\psi_i(q_i)$ of the ith agent ($i \in \mathcal{V}$) and the average formation output $\psi_{ave}(q)$ of all agents, we have

$$\delta_i(t) = \psi_i(q_i(t)) - \psi_{ave}(q(t)) = \frac{1}{N}\sum_{j=1}^{N}(\psi_i(q_i(t)) - \psi_j(q_j(t))).$$

With the desired formation objective (4), if we design the desired displacement deviation between $\psi_i(q_i^*)$ and $\psi_{ave}(q^*)$ as $\bar{\delta}_i^*$, where $q^* = \mathrm{col}(q_1^*, \cdots, q_N^*)$, then we have

$$\bar{\delta}_i^* = \lim_{t\to\infty} \delta_i(t) = \lim_{t\to\infty} \frac{1}{N}\sum_{j=1}^{N}(\psi_i(q_i(t)) - \psi_j(q_j(t))) = \frac{1}{N}\sum_{j=1}^{N}\delta_{ij}^*.$$

Based on the displacement deviation $\delta_i(t)$, the following theorem is given.

Theorem 3.1. *If $q^* = col(q_1^*, \cdots, q_N^*)$ satisfies*

$$\|\psi_i(q_i^*) - \psi_j(q_j^*) - \delta_{ij}^*\|_{P_i}^2 = 0, \quad i, j \in \mathcal{V}, \tag{6}$$

then

$$\|\psi_i(q_i^*) - \psi_{ave}(q^*) - \bar{\delta}_i^*\|_{P_i}^2 = 0, \quad i \in \mathcal{V}, \tag{7}$$

vice versa.

Proof. It should be noted that we assume that there must be at least one state $q^* = \text{col}(q_1^*, \cdots, q_N^*)$ in which the formation objective (6) can be met. Otherwise, the formation problem will be meaningless.

On one hand, if q^* satisfies (6), then $\psi_i(q_i^*) - \psi_j(q_j^*) - \delta_{ij}^* = 0$, $\forall i \in \mathcal{V}$. That is

$$\begin{cases} \psi_i(q_i^*) - \psi_1(q_1^*) - \delta_{i1}^* = 0, \\ \qquad\qquad \cdots \\ \psi_i(q_i^*) - \psi_N(q_N^*) - \delta_{iN}^* = 0. \end{cases}$$

Sum the above equations, we have

$$\psi_i(q_i^*) - \frac{1}{N}\sum_{j=1}^{N}(\psi_j(q_j^*) + \delta_{ij}^*) = 0, \quad i \in \mathcal{V},$$

which means (7) is satisfied.

On the other hand, the fact q^* satisfied (7) means that

$$\begin{aligned} &\psi_i(q_i^*) - \psi_{ave}(q^*) - \bar{\delta}_i^* = 0, \\ &\psi_j(q_j^*) - \psi_{ave}(q^*) - \bar{\delta}_j^* = 0, \quad \forall i, j \in \mathcal{V}. \end{aligned} \tag{8}$$

Make a difference between $\psi_i(q_i^*)$ and $\psi_j(q_j^*)$, then, we get

$$\psi_i(q_i^*) - \psi_j(q_j^*) - (\bar{\delta}_i^* - \bar{\delta}_j^*) = 0.$$

By the definition of $\bar{\delta}_i^*$, we have $\bar{\delta}_i^* - \bar{\delta}_j^* = \frac{1}{N}\sum_{k=1}^{N}(\delta_{ik}^* - \delta_{jk}^*) = \frac{1}{N}\sum_{k=1}^{N}\delta_{ij}^* = \delta_{ij}^*$, which means that (6) is accomplished. □

With Theorem (3.1), the minimum point of (5) for the ith agent ($i \in \mathcal{V}$) is equivalent to the minimum point of

$$V_i(\psi_i(q_i), \psi_{ave}(q)) = \frac{1}{2}(\|\psi_i(q_i) - \psi_{ave} - \bar{\delta}_i^*\|_{P_i}^2 + \|\psi_i(q_i) - \beta^*\|_{Q_i}^2), \tag{9}$$

where the constant vector β^* is predefined according to the specific requirements.

Above all, our task is to design a distributed controller for the ith ($i \in \mathcal{V}$) agent by using its own information q_i, $\hat{\eta}_i$ and the estimation $\hat{\eta}_j$ from its neighbor $j \in \mathcal{N}(i)$, such that the ith agent's system state $q_i(t)$ converges to q^* as $t \to \infty$, where q^* is the minimum point of (9). The formation control problem is summarized as follows:

Problem 3.1. *Consider N agents described by (2) communicating in an undirected connected topology $\mathcal{G}$. For the ith ($i \in \mathcal{V}$) agent, design a distributed controller $u_i(q_i, \hat{\eta}_i, \hat{\eta}_{\mathcal{N}(i)})$, $\hat{\eta}_{\mathcal{N}(i)} = (\hat{\eta}_j, j \in \mathcal{N}(i))$ such that the ith closed-loop system from the given initial state $q_i(0)$ asymptotically converges to the minimum point q_i^* of the value function* (9).

To find a solution of Problem 3.1, we refer to Theorem 3.9 and Theorem 4.8 in [47]. Then, the following Lemma is given.

Lemma 3.1. *A state $q^* = col(q_1^*, \cdots, q_N^*)$ is a solution to (9) if and only if*

$$\nabla_{q_i \in \mathbb{R}^m} V_i(\psi_i(q_i^*), \psi_{ave}(q^*)) = 0_m, \quad i \in \mathcal{V}. \tag{10}$$

4. Distributed algorithms and Convergence Analysis

In this section, two different distributed controllers are designed to solve Problem 3.1. One controller focuses on maintaining the PH structure for simplicity in stability analysis, while the other emphasizes a guaranteed convergence rate. Then, the convergence of the corresponding multi-agent systems is analyzed, respectively.

With the definition of the value function $V_i(q_i, \psi_{ave}(q))$ in Problem 3.1, the following maps are defined.

$$\begin{aligned} &F_i(q_i, \psi_{ave}(q)) := \nabla_{q_i} V_i(q_i, \psi_{ave}(q)), \\ &G_i(q_i, \hat{\eta}_i) := F_i(q_i, \psi_{ave}(q))|_{\psi_{ave}(q)=\hat{\eta}_i}, \end{aligned} \tag{11}$$

where $\hat{\eta}_i \in \mathbb{R}^l$. Define

$$\begin{aligned} F(q) &:= \mathrm{col}(F_1(q_1, \psi_{ave}(q)), \cdots, F_N(q_N, \psi_{ave}(q))), \\ G(q, \hat{\eta}) &:= \mathrm{col}(G_1(q_1, \hat{\eta}_1), \cdots, G_N(q_N, \hat{\eta}_N)), \end{aligned}$$

where $\hat{\eta} = \mathrm{col}(\hat{\eta}_1, \cdots, \hat{\eta}_N) \in \mathbb{R}^{Nl}$.

4.1. PH structure preserving distributed controller

In this subsection, we consider the specific example proposed in Section 3.1. In this case, $\psi_i(q_i) = q_i$. With the definition in (11) and let $\alpha = \frac{N-1}{N}$, we have

$$G_i(q_i, \hat{\eta}_i) = (\alpha P_i + Q_i)q_i - \alpha P_i \hat{\eta}_i - (\alpha P_i \bar{\delta}_i^* + Q_i \beta^*). \tag{12}$$

For the ith ($i \in \mathcal{V}$) agent, design the closed-loop system as

$$\begin{bmatrix} \dot{q}_i \\ \dot{p}_i \\ \dot{\hat{\eta}}_i \\ \dot{s}_i \end{bmatrix} = (J_{di} - R_{di}) \begin{bmatrix} \frac{\partial H_{cli}(q_i, p_i, \hat{\eta}_i, s_i)}{\partial q_i} \\ \frac{\partial H_{cli}(q_i, p_i, \hat{\eta}_i, s_i)}{\partial p_i} \\ \frac{\partial H_{cli}(q_i, p_i, \hat{\eta}_i, s_i)}{\partial \hat{\eta}_i} \\ \frac{\partial H_{cli}(q_i, p_i, \hat{\eta}_i, s_i)}{\partial s_i} \end{bmatrix}, \tag{13}$$

where the initial value $s_i(0) = 0_m$, $\hat{\eta}_i(0) = q_i(0)$[3], and $q_i(0)$, $p_i(0)$ are the given initial states of the agent $i \in \mathcal{V}$, the structure matrix J_{di} and the dissipation matrix R_{di} are

$$J_{di} = \begin{bmatrix} 0 & 0 & 0 & J_{d1i} \\ 0 & 0 & 0 & 0 \\ 0 & 0 & 0 & I \\ -J_{d1i}^\top & 0 & -I & 0 \end{bmatrix}, \quad R_{di} = \begin{bmatrix} I & 0 & 0 & 0 \\ 0 & I & 0 & 0 \\ 0 & 0 & I + ((\alpha P_i)^{-1} Q_i)^\top & 0 \\ 0 & 0 & 0 & R_{di1} \end{bmatrix},$$

with $J_{d1i} = -(\alpha P_i + Q_i)^{-1}(\alpha P_i)$, $R_{di1} = I + ((\alpha P_i + Q_i)^{-1}(\alpha P_i))^T$ and the *Hamiltonian* function

$$\begin{aligned} H_{cli} = &\frac{1}{2} G_i(q_i, \hat{\eta}_i)^\top G_i(q_i, \hat{\eta}_i) + \frac{1}{2} \sum_{j \in \mathcal{N}(i)} (\hat{\eta}_i - \hat{\eta}_j)^\top (\hat{\eta}_i - \hat{\eta}_j) \\ &+ \frac{1}{2} p_i^\top p_i + \frac{1}{2} (q_i - \hat{\eta}_i - s_i)^\top (q_i - \hat{\eta}_i - s_i), \quad i \in \mathcal{V}. \end{aligned} \tag{14}$$

Since P_i and Q_i are positive definite matrices, we have the structure matrix $J_{d1i} = -J_{d1i}^\top$ and the dissipation matrix $R_{di1} = R_{di1}^\top > 0$. Hence, the closed-loop system (13) maintains the PH structure.

By the closed-loop system (13), the system trajectory $q_i^*(t)$ can be obtained. Subsequently, the momentum $p_i^*(t)$ can be calculated according to the coupling relationship between displacement and momentum in mechanical systems. With the PH dynamic (2), the controller is implemented as

$$u_i(t) = \tilde{g}_i(q_i^*(t), p_i^*(t))^\dagger (\dot{p}_i^*(t) - C_i \frac{\partial H_i(q_i^*(t), p_i^*(t))}{\partial q_i^*(t)} - D_i \frac{\partial H_i(q_i^*(t), p_i^*(t))}{\partial p_i^*(t)}). \tag{15}$$

[3]The initial value of $\hat{\eta}_i(0)$ can be chosen arbitrarily. Considering the meaning of $\hat{\eta}_i$ is the ith agent's ($i \in \mathcal{V}$) estimation of the average formation output, we use its own position $q_i(0)$ as the first estimation.

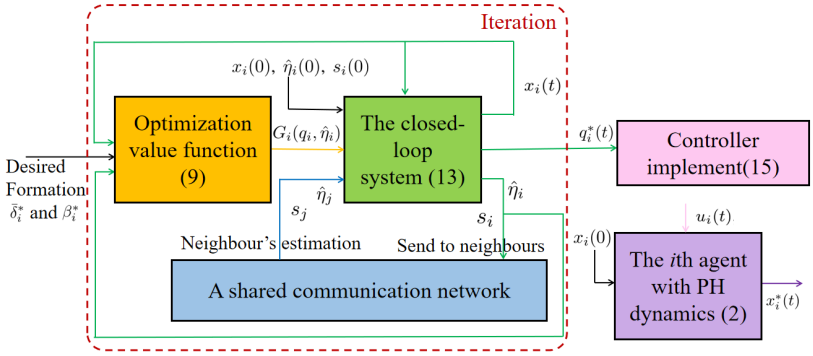

Figure 3: The control scheme of the ith agent ($i \in \mathcal{V}$).

By comparing the state $X_i = \text{col}(q_i, p_i, \hat{\eta}_i, s_i)$ in the closed-loop system (13) and the system state $x_i = \text{col}(q_i, p_i)$ in the PH system (2), one can observe that different from the inherent state characteristics of the ith agent system (the position q_i and the momentum p_i), the state $\hat{\eta}_i$ and s_i as the interconnected variables represent the interconnection relationship between multi-agent systems, similar to virtual springs [21]. The control scheme is shown in Fig.3. First, the desired formation parameters $\bar{\delta}_i^*, \beta^*$ and the initial value $x_i(0) = \text{col}(q_i(0), p_i(0))$, $\hat{\eta}_i(0)$, $s_i(0) = 0_l$ are given. Then, with the value function (9), the gradient $G_i(q_i, \hat{\eta}_i)$ is calculated and input into the closed-loop system as the desired direction of change for the system position q_i and $\hat{\eta}_i$. Getting the estimation $\hat{\eta}_j$ from neighbor $j \in \mathcal{N}(i)$, the system state X_i of agent $i \in \mathcal{V}$ is updated by (13). The updated estimation $\hat{\eta}_i$ and the error auxiliary variables are sent to its neighbors through a shared communication network. Finally, the state of the closed-loop system (13) converges to its equilibrium $X_i^* = \text{col}(q_i^*, p_i^*, \hat{\eta}_i^*, s_i^*)$. With the desired trajectory $q_i^*(t)$, the controller (15) is obtained. By inserting (15) into the PH system (2), the equilibrium x_i^* of the ith PH system (2) satisfies the formation objective.

Define $P = \text{diag}(P_1, \cdots, P_N)$, $Q = \text{diag}(Q_1, \cdots, Q_N)$, $p = \text{col}(p_1, \cdots, p_N)$, $s = \text{col}(s_1, \cdots, s_N)$. Then we have the compact form of (13):

$$\begin{bmatrix} \dot{q} \\ \dot{p} \\ \dot{\hat{\eta}} \\ \dot{s} \end{bmatrix} = (J_d - R_d) \begin{bmatrix} \frac{\partial H_{cl}(q,p,\hat{\eta},s)}{\partial q} \\ \frac{\partial H_{cl}(q,p,\hat{\eta},s)}{\partial p} \\ \frac{\partial H_{cl}(q,p,\hat{\eta},s)}{\partial \hat{\eta}} \\ \frac{\partial H_{cl}(q,p,\hat{\eta},s)}{\partial s} \end{bmatrix}, \tag{16}$$

where the structure matrix J_d and the dissipation matrix R_d are

$$J_d = \begin{bmatrix} 0 & 0 & 0 & J_{d1} \\ 0 & 0 & 0 & 0 \\ 0 & 0 & 0 & I \\ -J_{d1}^\top & 0 & -I & 0 \end{bmatrix}, \quad R_d = \begin{bmatrix} I & 0 & 0 & 0 \\ 0 & I & 0 & 0 \\ 0 & 0 & I + ((\alpha P)^{-1} Q)^\top & 0 \\ 0 & 0 & 0 & R_{d1} \end{bmatrix}, \tag{17}$$

with $J_{d1} = (\alpha P + Q)^{-1}(-\alpha P)$, $R_{d1} = I + (\alpha P)^\top (\alpha P + Q)^{-T}$ and the total *Hamiltonian* function

$$H_{cl} = \frac{1}{2} G(q, \hat{\eta})^\top G(q, \hat{\eta}) + \frac{1}{2} p^\top p + \frac{1}{2} \hat{\eta}^\top (L \otimes I_n) \hat{\eta} + \frac{1}{2} (q - \hat{\eta} + s)^\top (q - \hat{\eta} + s). \tag{18}$$

It is easy to verify that when $P_i, Q_i > 0$ holds in the formation goal (9), the dissipation matrix $R_d = R_d^\top \geq 0$ and the structure matrix $J_d = -J_d^\top$ in (17). Hence, the structure of PH systems is maintained.

Theoretically, the fact that the distributed controller (15) is a solution to Problem 3.1 implies that, under the action of this controller, the system state of agent $i \in \mathcal{V}$ in (2) converges to the equilibrium of system (13). Meanwhile, at this equilibrium X_i^*, the value function (9) reaches its minimum value, where the formation objective is achieved. The following two theorems, with detailed theoretical derivations and analysis, illustrate these points. Specifically, The first is a convergence analysis of the closed-loop system (16).

Theorem 4.1. *The PH system* (16) *is asymptotically convergent to an equilibrium point* $X^* = (q^*, p^*, \hat{\eta}^*, s^*)$ *which belongs to the invariant set*

$$S = \{X = col(q, p, \hat{\eta}, s) | G(q, \hat{\eta}) = 0, q - \hat{\eta} + s = 0, p = 0, (L \otimes I_m)\hat{\eta} = 0, (1_N^\top \otimes I_m)s = 0_{Nm}\}. \tag{19}$$

Proof. With the property of the PH structure of system (16), directly choosing the *Hamiltonian* function $H_{cl} \geq 0$ in (18) as a candidate Lyapunov function. The time derivative of H_{cl} is

$$\dot{H}_{cl} = -(\frac{\partial H_{cl}}{\partial X})^\top R_d \frac{\partial H_{cl}}{\partial X}. \tag{20}$$

It follows that $\dot{H}_{cl} \leq 0$. Recalling LaSalle's invariance principle, system (16) asymptotically converges to the largest invariant set

$$S = \{X | \frac{\partial H_{cl}}{\partial X} = 0\}.$$

Then we are going to analysis the elements $X \in S$. Based on (12), we have the gradient of $G_i(q_i, \hat{\eta}_i)$ with respect to q_i and $\hat{\eta}_i$ respectively represented as

$$\begin{aligned} \frac{\partial G_i(q_i, \hat{\eta}_i)}{\partial q_i} &= \alpha P_i + Q_i, \\ \frac{\partial G_i(q_i, \hat{\eta}_i)}{\partial \hat{\eta}_i} &= -\alpha P_i. \end{aligned} \tag{21}$$

Inserting (12), (16) and (21) into (20), we have

$$\dot{H}_{cl} = -\|(\alpha P + Q)^\top G + q - \hat{\eta} + s\|^2 - \|p\|^2 - \|q - \hat{\eta} + s\|^2 - \|(L \otimes I_m)\hat{\eta} - (q - \hat{\eta} + s)\|^2.$$

Since $(\alpha P + Q)^\top > 0$, then $\dot{H}_{cl} = 0$ if and only if $G(q, \hat{\eta}) = 0$, $q - \hat{\eta} + s = 0$, $p = 0$, $(L \otimes I_m)\hat{\eta} = 0$. Noticing that $(1_N^\top \otimes I_m)\dot{s} = 0$ and $s(0) = 0_{Nm}$, we have $(1_N^\top \otimes I_m)s(t) = 0, \forall t \geq 0$.

Hence, the PH system (16) asymptotically converges to the set S in (19). □

Then, the relationship of the equilibrium X^* of the PH system (16) and the minimum point q^* of the value function (9) is summarized as follows.

Theorem 4.2. *If* $X^* = col(q^*, p^*, \hat{\eta}^*, s^*)$ *is an equilibrium of the PH system* (16)*, then* q^* *is one of the minimum point of the value function* (9) *where the formation goal* (4) *is achieved.*

Proof. If X^* is an equilibrium of (16), then by Theorem 4.1, we have $X^* \in S$ that means

$$\begin{cases} G(q^*, \hat{\eta}^*) = 0_{Nm}, \\ q^* - \hat{\eta}^* + s^* = 0_{Nm}, \\ (L \otimes I_m)\hat{\eta}^* = 0_{Nm}, \\ p^* = 0_{Nm_p}, \\ (1_N^\top \otimes I_m)s = 0_{Nm}. \end{cases} \tag{22}$$

As the Laplacian matrix of $\mathcal{G}$, L has and only has one 0 eigenvalue, with the corresponding eigenvector 1_N. The third formula in (22) implies that $\hat{\eta}^* = \tilde{\alpha} 1_N$, $\tilde{\alpha} \in \mathbb{R}$. Therefore, $\hat{\eta}_i^* = \hat{\eta}_j^*$, $\forall i, j \in \mathcal{V}$. Noticing that $(1_N^\top \otimes I_m)s = 0, \forall t \geq 0$ and $q^* - \hat{\eta}^* + s^* = 0$, we have $(1_N^\top \otimes I_m)(q^* - \hat{\eta}^*) = (1_N^\top \otimes I_m)q^* - (1_N^\top \otimes I_m)\hat{\eta}^* = 0$. It indicates that $\sum_{i=1}^N \hat{\eta}_i^* = N q_{ave}^*$, where $q_{ave}^* = \frac{1}{N}\sum_{i=1}^N q_i^*$. Above all, for any $i \in \mathcal{V}$, $F_i(q_i^*, q_{ave}^*)|_{q_{ave}^* = \hat{\eta}_i^*} = G_i(q_i^*, \hat{\eta}_i^*) = 0$. With the help of Lemma 3.1, the proof is completed. □

By Theorem 4.1 and Theorem 4.2, the PH system (16) asymptotically converges to the equilibrium X^* where the desired formation is achieved.

4.2. The second distributed controller

In this subsection, another controller is proposed. The goal of this controller is to solve Problem 3.1 by utilizing the formation output $\psi_i(q_i)$. There is a significant difference compared to the previous subsection. Under the action of the controller proposed here, the PH structure of the closed-loop system will be disrupted. However, we manage to find a suitable Lyapunov function. By using this Lyapunov function, we proved the exponential stability of the corresponding closed-loop system.

Assumption 1. *Assume that the gradient $F(q)$ of the value function* (9) *is w-strongly monotone and L_f-Lipschitz. The formation output $\psi(q)$ and the mapping $G(q,\hat{\eta})$ are L_ψ-Lipschitz and L_g-Lipschitz, respectively, where $\psi(q) = col(\psi_1(q_1),\cdots,\psi_N(q_N))$.*

This assumption is general in aggregative games, such as in [12, 11]. For example, this assumption is satisfied if we let $\psi_i(q_i) = K_i q_i + b_i$ with the matrix $K_i > 0$ and an arbitrary constant vector b_i, then with the definition of $V_i(q_i, \psi_{ave}(q))$ in (9), the assumption is satisfied.

Similar to Section 4.1, we first design a closed-loop system as

$$\begin{cases} \dot{q}_i = v_i, \\ \dot{v}_i = -k_1 v_i - k_2 G_i(q_i,\hat{\eta}_i), \\ \dot{\hat{\eta}}_i = \psi_i(q_i) - \hat{\eta}_i - \gamma\sum_{j\in\mathcal{N}(i)}(\hat{\eta}_i - \hat{\eta}_j) - z_i, \\ \dot{z}_i = \gamma\sum_{j\in\mathcal{N}(i)}(\hat{\eta}_i - \hat{\eta}_j), \end{cases} \tag{23}$$

where $\hat{\eta}_i(0) = q_i(0), z_i(0) = 0_l$, $v_i(0)$ can be chosen arbitrarily, and the parameters γ, k_1, k_2 will be determined later.

From a physical perspective, q_i represents the position of agent $i \in \mathcal{V}$, while v_i represents velocity as the derivative of q_i. The change in velocity is related to itself and the mapping $G_i(q_i,\hat{\eta}_i)$. The update of the estimation $\hat{\eta}_i$ of the ith agent is dependent on three parts: (1) the difference between the ith agent's estimation $\hat{\eta}_i$ and its own formation output $\psi_i(q_i)$; (2) the total difference between $\hat{\eta}_i$ and the estimation $\hat{\eta}_j$ from its neighbor $j \in \mathcal{N}(i)$; (3) negative feedback term z_i. The final formula of (23) serves as an integrator to eliminate the error. As the system runs, the desired system trajectory $q_i^{**}(t)$ can be obtained, after which the corresponding controller can be implemented.

Remark 4. *The closed-loop system* (23) *cannot maintain PH structure. This is due to the mapping $\psi_i(q_i)$ such that the structure matrix J_{di} and the dissipation matrix R_{di} may not satisfy the anti-symmetric or positive-definite conditions.*

By the system (23), the desired trajectory $q_i^{**}(t)$ is obtained. Further, p_i^{**} and $\dot{p}_i^{**}$ are got according to the coupling relationship between position and momentum in mechanical systems. Then we can solve the second controller as

$$u_i(t) = \tilde{g}_i(q_i^{**}(t), p_i^{**}(t))^{\dagger}(\dot{p}_i^{**}(t) - D_i\frac{\partial H_i(q_i^{**}(t), p_i^{**}(t))}{\partial p_i^{**}(t)} - C_i\frac{\partial H_i(q_i^{**}(t), p_i^{**}(t))}{\partial q_i^{**}(t)}). \tag{24}$$

Let $v = \mathrm{col}(v_1,\cdots,v_N)$, $z = \mathrm{col}(z_1,\cdots,z_N)$, we rewrite (23) in a compact form:

$$\begin{cases} \dot{q} = v, \\ \dot{v} = -k_1 v - k_2 G(q,\hat{\eta}), \\ \dot{\hat{\eta}} = \psi(q) - \hat{\eta} - \gamma(L\otimes I_l)\hat{\eta} - z, \quad \hat{\eta}(0) = q(0), \\ \dot{z} = \gamma(L\otimes I_l)\hat{\eta}, \quad z(0) = 0_{Nl}. \end{cases} \tag{25}$$

To make our control methods more comprehensible, the flow diagram is given as Fig.4.

As can be seen from Fig.4, each agent calculates based on its own value function V_i and initial values $q_i(0)$, $v_i(0)$, $\hat{\eta}_i(0)$, $s_i(0)$. Then, it obtains $\hat{\eta}_j$ through information interaction with its neighbors $j \in \mathcal{N}(i)$. Further, the controller $u_i(t)$ is solved by (23). Substituting the controller (24) into the multi-agent systems (2), the achievement of the formation objective (4) will be proven. First, the following theorem is given to analyze the convergence of system (25).

Theorem 4.3. *Under Assumption 1, the system (25) exponentially converges to the equilibrium point $(q^*, v^*, \hat{\eta}^*, z^*)$ with the designing parameters*

$$\begin{cases} k_1 \geq \varepsilon + \frac{wk_2}{4\varepsilon} + \frac{k_2 L_f^2}{w\varepsilon} + \frac{5N+4}{4N}L_\psi^2, \\ \gamma \geq \frac{8}{\lambda_2}, \\ k_2\varepsilon \leq \frac{w}{2L_g^2}, \quad k_2, \varepsilon > 0. \end{cases} \tag{26}$$

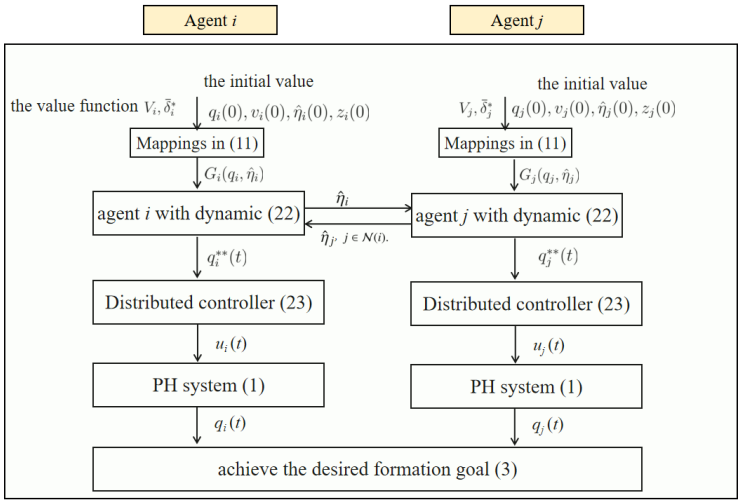

Figure 4: The flow diagram of our control method operations.

Proof. The equilibrium $(q^*, v^*, \hat{\eta}^*, z^*)$ of (25) satisfies that:

$$\begin{cases} q^* = 0_{Nm}, \\ -k_1 v^* - k_2 G(q^*, \hat{\eta}^*) = 0_{Nm}, \\ \psi(q^*) - \hat{\eta}^* - \gamma(L \otimes I_l)\hat{\eta}^* - z^* = 0_{Nl}, \\ \gamma(L \otimes I_l)\hat{\eta}^* = 0_{Nl}. \end{cases} \tag{27}$$

Let $\bar{q} = q - q^*$, $\bar{v} = v - v^*$, $\bar{\eta} = \hat{\eta} - \hat{\eta}^*$ and $\bar{z} = z - z^*$. Make a difference between (25) and (27), we have the following system by the decomposition of the Laplacian matrix L.

$$\begin{cases} \dot{\bar{q}} = \bar{v}, \\ \dot{\bar{v}} = -k_1 \bar{v} - k_2 \bar{G}(q, \hat{\eta}), \\ \dot{\bar{\eta}} = -\bar{\eta} - \gamma(L \otimes I_l)\bar{\eta} - \bar{z} - (rr^T \otimes I_l)\dot{\bar{\psi}}(q), \\ \dot{\bar{z}} = \gamma(L \otimes I_l)\bar{\eta} - (RR^T \otimes I_l)\dot{\bar{\psi}}(q). \end{cases} \tag{28}$$

where $\bar{G}(q, \hat{\eta}) = G(q, \hat{\eta}) - G(q^*, \hat{\eta}^*)$, $\bar{\psi}(q) = \psi(q) - \psi(q^*)$, $r = \frac{1}{\sqrt{N}} 1_N$, $r^\top R = 0_N^T$, $R^\top R = I_{N-1}$, $RR^\top = I_N - \frac{1}{N} 1_N 1_N^\top$.

Then, our task is to prove $\bar{q} \to 0$ $(q \to q^*)$. Through the orthogonal transformation of r and R:

$$\begin{aligned} \tilde{\eta} &= \mathrm{col}(\tilde{\eta}_1, \tilde{\eta}_2) = ([r \quad R]^\top \otimes I_l)\bar{\eta}, \\ \tilde{z} &= \mathrm{col}(\tilde{z}_1, \tilde{z}_2) = ([r \quad R]^\top \otimes I_l)\bar{z}, \end{aligned}$$

where $\tilde{\eta}_1, \tilde{z}_1 \in \mathbb{R}^l$, $\tilde{\eta}_2, \tilde{z}_2 \in \mathbb{R}^{(N-1)l}$. After that, Eq. (28) is rewritten as

$$\begin{cases} \dot{\bar{q}} = \bar{v}, \\ \dot{\bar{v}} = -k_1 \bar{v} - k_2 \bar{G}(q, \hat{\eta}) \\ \dot{\tilde{\eta}}_1 = -\tilde{\eta}_1 - (r^\top \otimes I_l)\dot{\bar{\psi}}(q), \\ \dot{\tilde{\eta}}_2 = -\tilde{\eta}_2 - \tilde{z}_2 - \gamma(R^\top L R \otimes I_l)\tilde{\eta}_2, \\ \dot{\tilde{z}}_1 = 0, \\ \dot{\tilde{z}}_2 = \gamma(R^\top L R \otimes I_l)\tilde{\eta}_2 - (R^\top \otimes I_l)\dot{\bar{\psi}}(q). \end{cases} \tag{29}$$

The Lyapunov function is taken as

$$V = V_1 + V_2 + V_3$$

where

$$V_1 = \frac{1}{2}\|\varepsilon\bar{q} + \bar{v}\|^2 + \frac{1}{2}(\varepsilon(k_1 - \varepsilon))\|\bar{q}\|^2, \varepsilon > 0,$$
$$V_2 = \|\tilde{\eta}_1\|^2, \quad V_3 = \frac{1}{2}\|\tilde{\eta}_2\|^2 + \frac{1}{2}\|\tilde{\eta}_2 + \tilde{z}_2\|^2.$$

The derivative of V_1 along (29) is

$$\begin{aligned}\dot{V}_1 &= (\varepsilon\bar{q} + \bar{v})^\top(\varepsilon\bar{v} - k_1\bar{v} - k_2\bar{G}(q,\hat{\eta})) + \varepsilon(k_1 - \varepsilon)\bar{q}^\top\bar{v},\\ &= -k_2\varepsilon\bar{q}^\top\bar{G}(q,\hat{\eta}) - (k_1 - \varepsilon)\|\bar{v}\|^2 - k_2\bar{v}^\top\bar{G}(q,\hat{\eta}).\end{aligned}$$

According to Assumption 1, due to the w-strongly monotone of $F(q)$ and L_f-Lipschitz of $G(q,\hat{\eta})$, the first term of $\dot{V}_1$ can be scaled down to

$$\begin{aligned}-k_2\varepsilon\bar{q}^\top\bar{G}(q,\hat{\eta}) &= -k_2\varepsilon(q - q^*)^\top(G(q,\hat{\eta}) - G(x^*,\hat{\eta}^*))\\ &= -k_2\varepsilon(q - q^*)^\top(G(q,\hat{\eta}) - G(q,\hat{\eta}^*)) - k_2\varepsilon(q - q^*)^\top(F(q) - F(q^*))\\ &\le k_2\varepsilon L_g\|\bar{q}\|\|\bar{\eta}\| - k_2\varepsilon w\|\bar{q}\|^2 \le -\frac{3}{4}k_2\varepsilon w\|\bar{q}\|^2 + \frac{k_2\varepsilon L_g^2}{w}\|\bar{\eta}\|^2.\end{aligned}$$

Similarly, the third term of $\dot{V}_1$ is scaled down to

$$\begin{aligned}&k_2\bar{v}^\top\bar{G}(q,\hat{\eta}) = k_2(v - v^*)^\top(G(q,\hat{\eta}) - G(q^*,\hat{\eta}^*))\\ &= k_2(v - v^*)^\top(G(q,\hat{\eta}) - G(q,\hat{\eta}^*)) + k_2(v - v^*)^\top(F(q) - F(q^*))\\ &\le k_2L_g\|\bar{\eta}\|\|\bar{v}\| + k_2L_f\|\bar{q}\|\|\bar{v}\| \le \frac{L_g^2k_2\varepsilon}{w}\|\bar{\eta}\|^2 + \frac{k_2\varepsilon w}{4}\|\bar{q}\|^2 + (\frac{wk_2}{4\varepsilon} + \frac{k_2L_f^2}{w\varepsilon})\|\bar{v}\|^2.\end{aligned}$$

Hence, $\dot{V}_1$ is scaled down to

$$\dot{V}_1 \le -(k_1 - \varepsilon - \frac{wk_2}{4\varepsilon} - \frac{k_2L_f^2}{w\varepsilon})\|\bar{v}\|^2 - \frac{k_2\varepsilon w}{2}\|\bar{q}\|^2 + \frac{2L_g^2k_2\varepsilon}{w}\|\bar{\eta}\|^2.$$

Under Assumption 1, due to the L_ψ-Lipschitz of $\psi(q)$, the derivative of V_2 along (29) is

$$\dot{V}_2 = 2\tilde{\eta}_1^\top(-\tilde{\eta}_1 - (r^\top \otimes I_n)\dot{\tilde{\psi}}(q)) \le -2\|\tilde{\eta}_1\|^2 - \frac{2L_\psi}{\sqrt{N}}\|\tilde{\eta}_1\|\|\bar{v}\| \le -\|\tilde{\eta}_1\|^2 + \frac{L_\psi^2}{N}\|\bar{v}\|^2,$$

and the derivative of V_3 along (29) is

$$\begin{aligned}\dot{V}_3 &= \tilde{\eta}_2^\top(-\tilde{\eta}_2 - \tilde{z}_2 - \gamma(R^\top LR \otimes I_l)\tilde{\eta}_2) + (\tilde{\eta}_2 + \tilde{z}_2)^\top(-\tilde{\eta}_2 - \tilde{z}_2 - (R^\top \otimes I_l)\dot{\tilde{\psi}}(q))\\ &= -2\|\tilde{\eta}_2\|^2 - \|\tilde{z}_2\|^2 - 3\tilde{\eta}_2^\top\tilde{z}_2 - \gamma\tilde{\eta}_2^\top(R^\top LR \otimes I_l)\tilde{\eta}_2 - \tilde{\eta}_2^T(R^\top \otimes I_n)\dot{\tilde{\psi}}(q) - \tilde{z}_2^\top(R^\top \otimes I_n)\dot{\tilde{\psi}}(q).\end{aligned}$$

For the undirected connected $\mathcal{G}$, only the minimum eigenvalue λ_1 of matrix L is equal to 0, the others $0 < \lambda_2 < \cdots < \lambda_N$ such that

$$-\tilde{\eta}_2^\top(R^\top LR \otimes I_n)\tilde{\eta}_2 \le -\lambda_2\|\tilde{\eta}_2\|^2. \tag{30}$$

By $ab \le \frac{1}{2c}a^2 + \frac{c}{2}b^2$, $c > 0$, we have

$$\begin{aligned}&-\tilde{\eta}_2^\top(R^\top \otimes I_n)\dot{\tilde{\psi}}(q) \le \|\tilde{\eta}_2\|^2 + \frac{L_\psi^2}{4}\|\bar{v}\|^2,\\ &-\tilde{z}_2^\top(R^\top \otimes I_n)\dot{\tilde{\psi}}(q) \le \frac{1}{4}\|\tilde{z}_2\|^2 + L_\psi^2\|\bar{v}\|^2,\\ &-3\tilde{\eta}_2^\top\tilde{z}_2 \le 3\|\tilde{z}_2\|\|\tilde{\eta}_2\| \le \frac{1}{4}\|\tilde{z}_2\|^2 + 9\|\tilde{\eta}_2\|^2.\end{aligned} \tag{31}$$

It follows from (30) and (31) that

$$\dot{V}_3 \leq -(\gamma\lambda_2 - 8)\|\tilde{\eta}_2\|^2 + \frac{5}{4}L_\psi^2\|\bar{v}\|^2 - \frac{1}{2}\|z_2\|^2. \tag{32}$$

Then, the derivative of V along (29) can be calculated by the analysis above as

$$\begin{aligned}\dot{V} = \dot{V}_1 + \dot{V}_2 + \dot{V}_3 \leq -(k_1 - \varepsilon - \frac{wk_2}{4\varepsilon} - \frac{k_2L_f^2}{w\varepsilon} - \frac{5N+4}{4N}L_\psi^2)\|\bar{v}\|^2 - \frac{1}{2}\|z_2\|^2 \\ - \frac{k_2\varepsilon w}{2}\|\bar{q}\|^2 - (1 - \frac{2L_g^2k_2\varepsilon}{w})\|\bar{\eta}\|^2 - (\gamma\lambda_2 - 8)\|\tilde{\eta}_2\|^2.\end{aligned}$$

Let $\zeta_1 = k_1 - \varepsilon - \frac{wk_2}{4\varepsilon} - \frac{k_2L_f^2}{w\varepsilon} - \frac{5N+4}{4N}L_\psi^2$, $\zeta_2 = \frac{k_2w}{2\varepsilon}$, $\zeta_3 = 1 - \frac{2L_g^2k_2\varepsilon}{w}$, $\zeta_4 = \gamma\lambda_2 - 8$. If the parameters k_1, ε, k_2 satisfies the condition in (26), we have $\zeta_1, \zeta_2, \zeta_3, \zeta_4 \geq 0$. Noticing that $\|\bar{\eta}\|^2 = \|\tilde{\eta}_1\|^2 + \|\tilde{\eta}_2\|^2$ and $(a+b)^2 \leq 2(a^2+b^2)$, we have

$$\begin{aligned}\dot{V} &\leq -\zeta_1\|\bar{v}\|^2 - \frac{1}{2}\|z_2\|^2 - \zeta_2\|\varepsilon\bar{q}\|^2 - \zeta_3\|\tilde{\eta}_1\|^2 - \zeta_3\|\tilde{\eta}_2\|^2 - \zeta_4\|\tilde{\eta}_2\|^2 \\ &\leq -\frac{\zeta_5}{4}\|\varepsilon\bar{q} + \bar{v}\|^2 - \frac{\zeta_2 - \frac{\zeta_5}{2}}{\varepsilon^3(k_1-\varepsilon)}\varepsilon(k_1-\varepsilon)\|\bar{q}\|^2 - \zeta_3\|\tilde{\eta}_1\|^2 - \frac{\zeta_6}{2}\|z_2 + \tilde{\eta}_2\|^2 - \frac{2(\zeta_3+\zeta_4-\zeta_5)}{2}\|\tilde{\eta}_2\|^2 \\ &\leq -\zeta V,\end{aligned}$$

where $\zeta_5 = \min\{\zeta_1, \zeta_2\}$, $\zeta_6 = \min\{\frac{1}{4}, \frac{\zeta_3+\zeta_4}{2}\}$, $\zeta = \min\{\frac{\zeta_5}{2}, \frac{\zeta_2 - \frac{\zeta_5}{2}}{\varepsilon^3(k_1-\varepsilon)}, \zeta_3, \zeta_6, 2(\zeta_3+\zeta_4-\zeta_5)\}$. By the Lyapunov stability theorem, the proof is completed. □

Next, we will illustrate the relationship between the minimum point q^* of the value function (9) and the equilibrium point $(q^*, v^*, \hat{\eta}^*, z^*)$ that system (25) converges to.

Theorem 4.4. *Under Assumption 1, if there exists an equilibrium point $(q^*, v^*, \hat{\eta}^*, z^*)$ of the closed-loop system (25), then q^* is the minimum point of the value function (9). Conversely, there exists $v^* \in \mathbb{R}^{Nm}$, $\hat{\eta}^* \in \mathbb{R}^{Nn}$, $z^* \in \mathbb{R}^{Nn}$ such that $(q^*, v^*, \hat{\eta}^*, z^*)$ is an equilibrium of (25) if x^* is the minimum point of (9).*

Proof. If $(q^*, v^*, \hat{\eta}^*, z^*)$ is an equilibrium of system (25), then the conditions in (27) are satisfied, that is,

$$\begin{cases} v^* = 0_{Nm}, \\ G(q^*, \hat{\eta}^*) = 0_{Nm}, \\ \psi(q^*) - \hat{\eta}^* - z^* = 0_{Nl}, \\ (L \otimes I_l)\hat{\eta}^* = 0_{Nl}. \end{cases} \tag{33}$$

For the undirected connected communicate topology $\mathcal{G}$, we have $L1_N = 0_N$. Then by the last formula in (33), we have $(1_N^\top \otimes I_l)(L \otimes I_l)\hat{\eta} = 0_{Nl}$. Noticing that $z(0) = 0_{Nl}$, by (25) we have $(1_N^\top \otimes I_l)z^* = 0$. As a result of $(1_N^\top \otimes I_l)(\psi(q^*) - \hat{\eta}^*) = 0$ and $(L \otimes I_l)\hat{\eta}^* = 0_{Nl}$, we obtain $\hat{\eta}_i^* = \hat{\eta}_j^* = \psi_{ave}(q^*)$, where $i, j \in \mathcal{V}$. In consideration of the definition of $G(x^*, \hat{\eta}^*) = F(x^*)|_{\psi_{ave}(q^*)=\hat{\eta}_i^*}$, $G(x^*, \hat{\eta}^*) = 0_{Nm}$ indicates that $\nabla_{q_i}V_i(q_i^*, \psi_{ave}(q^*)) = 0_m$, for every $i \in \mathcal{V}$. Hence, by Lemma 3.1, q^* is the minimum point of the value function (9).

Conversely, if q^* is the minimum point of (9), by Lemma 3.1, we have $F_i(q_i^*, \psi_{ave}(q^*)) = 0_m$. If we choose $\hat{\eta}_i^* = \psi_{ave}(q^*)$ for any $i \in \mathcal{V}$, then we obtain $G(q^*, \hat{\eta}^*) = F(q^*)|_{\psi_{ave}(q^*)=\hat{\eta}_i^*} = 0_{Nm}$ and $(L \otimes I_l)\hat{\eta}^* = 0_{Nl}$. When we choose $v^* = 0_{Nm}$ and $z^* = \psi(q^*) - \hat{\eta}^*$, Eq. (27) is satisfied. The proof is completed. □

With the help of Theorem 4.3 and Theorem 4.4, the equilibrium of system (25) is the minimum point of the value function (9) in Problem 3.1 and further meets the requirements of formation control. Hence, the controller (24) is a solution to Problem 3.1.

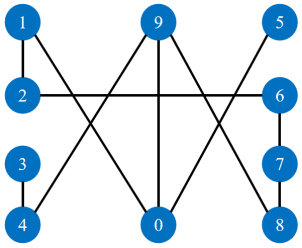

Figure 5: The communicate topology of 10 nonholonomic wheeled robots.

5. Simulation examples

This section presents simulations of a fleet of nonholonomic wheeled robots to illustrate the proposed controllers' effectiveness. The formation control goals are aligned with the motivational example mentioned in Section 3.1.

We consider N nonholonomic wheeled robots with $N = 10$ that are connected by an undirected graph as Fig.5.

As shown in Fig.6, the ith ($i \in [1{:}10]$) nonholonomic wheeled robot has a center of the axle $(X_{C,i}, Y_{C,i})$ and the heading is represented by ϕ_i. To model the ith ($i \in [1{:}10]$) wheeled robot system in PH form, we choose the system state as $x_i = \mathrm{col}(\tilde{q}_i, p_i') \in \mathbb{R}^6$, where $\tilde{q}_i = \mathrm{col}(q_i, \phi_i) \in \mathbb{R}^3$ is constituted by the position $q_i = \mathrm{col}(X_{C,i}, Y_{C,i}) \in \mathbb{R}^2$ and the angle $\phi_i \in \mathbb{R}$ between the x-axis and the heading direction, the momentum $p_i' \in \mathbb{R}^3$.

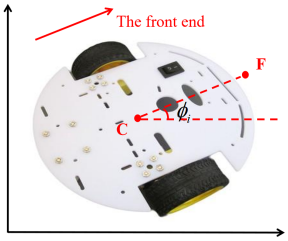

Figure 6: The structure diagram of the wheeled robot.

As a result of the coordinate transformation, the original rigid body momentum $p_i' \in \mathbb{R}^3$ is converted into three parts, including the sideward momentum $p_{i1} \in \mathbb{R}$, the forward momentum $p_{i2} \in \mathbb{R}$, and the angular momentum $p_{i3} \in \mathbb{R}$. Based on the new coordinates, the sideward momentum is eliminated, i.e., $p_{i3} = 0$. Hence, the dynamics of wheeled robot i with a nonholonomic constraint are given as [20]:

$$\begin{bmatrix} \dot{\tilde{q}}_i \\ \dot{p}_i \end{bmatrix} = \begin{bmatrix} 0 & J_i(\tilde{q}_i) \\ -J_i^T(\tilde{q}_i) & R_i \end{bmatrix} \begin{bmatrix} \frac{\partial H_i}{\partial \tilde{q}_i} \\ \frac{\partial H_i}{\partial p_i} \end{bmatrix} + \begin{bmatrix} 0 \\ I_2 \end{bmatrix} \tilde{u}_i, \tag{34}$$

with the dissipation matrix $R_i = J_i^T(\tilde{q}_i)\mathrm{diag}(R_{i1}, R_{i2}, R_{i3})J_i(\tilde{q}_i)$ and the *Hamiltonian* function $H_i = \frac{1}{2} p_i^T (M_i)^{-1} p_i$. The mass matrix M_i and the structure matrix $J_i(\tilde{q}_i)$ of robot i are $M_i = \begin{bmatrix} m_i & 0 \\ 0 & I_{cm,i} \end{bmatrix}$, $J_i(\tilde{q}_i) = \begin{bmatrix} \cos\phi_i & 0 \\ \sin\phi_i & 0 \\ 0 & 1 \end{bmatrix}$, in which the mass $m_i \in \mathbb{R}$, the rotational inertia $I_{cm,i} \in \mathbb{R}$. The vector $p_i = \mathrm{col}(p_{i1}, p_{i2}) \in \mathbb{R}^2$ is consistent with the forward momentum p_{i1} and the angular momentum p_{i2} of the ith ($i \in [1{:}10]$) robot.

Based on the motivational example, the square is designed with 4 vertices on $(-6, -6)$, $(6, -6)$, $(-6, 6)$ and $(6, 6)$, respectively. The formation goal is to form a pentagram shape near the center of the square $(0, 0)$. Hence, the value function of ith ($i \in [1{:}10]$) wheeled robot is designed as

$$V_i(q_i) = \frac{1}{2}\|q_i - \frac{1}{10}\sum_{i=1}^{10} q_i - \bar{\delta}_i^*\|_{P_i} + \frac{1}{2}\|q_i - \beta^*\|_{Q_i}. \tag{35}$$

Part of the system parameters of 10 agents are listed in Table 1. Besides, $\beta^* = (0,0)^\top$, $\hat{\eta}_i(0) = q_i(0)$, $P_i = \mathrm{diag}(100,100)$, $Q_i = \mathrm{diag}(0.1,0.1)$, $i \in [1{:}10]$. Ignore the damp so that $R_{ii} = 0, i \in [1{:}3]$. Above all, the optimization problem of general formation control is established.

	$m_i(kg)$	$r_i(m)$	$q_i(0)$	$\bar{\delta}_i^*$	$\phi_i(0)$
agent 1	0.1	0.1	$(-6,3)^\top$	$(-2.50,0.96)^\top$	0 rad
agent 2	0.3	0.2	$(-6,6)^\top$	$(-0.50,0.96)^\top$	π rad
agent 3	0.2	0.15	$(0,6)^\top$	$(0.00,2.96)^\top$	0 rad
agent 4	0.1	0.2	$(6,6)^\top$	$(0.50,0.96)^\top$	$\frac{\pi}{2}$ rad
agent 5	0.2	0.3	$(6,3)^\top$	$(2.50,0.96)^\top$	$\frac{\pi}{3}$ rad
agent 6	0.3	0.25	$(6,0)^\top$	$(0.90,-0.34)^\top$	$\frac{\pi}{2}$ rad
agent 7	0.1	0.3	$(6,-6)^\top$	$(1.50,-2.54)^\top$	$-\pi$ rad
agent 8	0.3	0.1	$(0,-6)^\top$	$(0.00,-1.04)^\top$	$\frac{\pi}{6}$ rad
agent 9	0.1	0.15	$(-6,-6)^\top$	$(-1.50,-2.54)^\top$	$-\frac{\pi}{2}$ rad
agent 0	0.2	0.2	$(-6,0)^\top$	$(-0.90,-0.34)^\top$	0 rad

Table 1: Parameters of 10 wheeled robots.

5.1. *Simulations of system* (16) *(preserving the PH structure)*

Based on the PH dynamic (34) and the value function (35), the closed-loop system (16) is used to obtain the desired system trajectory, and then the controller is obtained based on (15).

5.1.1. *Simulation results*

The evolutions of the ith ($i \in \mathcal{V}$) agent's position trajectory $X_{C,i}$ and $Y_{C,i}$ are shown in Fig.7 and Fig.8, respectively.

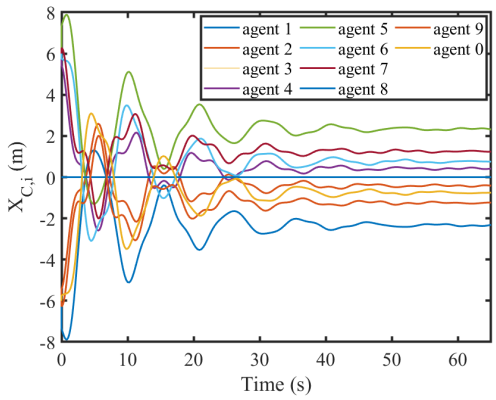

Figure 7: The evolutions of $X_{C,i}$ of system (16).

The position of 10 agents at different times is given as Fig.9. In this figure, we can find that these 10 agents begin at $t = 0s$. At $t = 10s$, a rough pentagram shape was formed. Then, after adjustment, the target pentagram was reached. Fig. 10 shows the changing of the *Hamiltonian* function H_{cl}. At around 40s, $H_{cl} \to 0$ implies that the system (16) converges to the equilibrium.

5.1.2. *The controller implementation*

With system (16), we got the target position trajectory $q_i^*(t)$. By Fig. 7 and Fig.8, the curves of $X_{C,i}^*(t)$ and $Y_{C,i}^*(t)$ are obtained. With the system dynamic (34) of the ith ($i \in [1{:}10]$) wheeled robot, the forward momentum p_{i1} and the

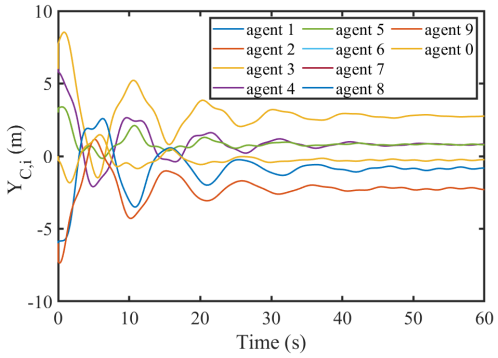

Figure 8: The evolutions of $Y_{C,i}$ of system (16).

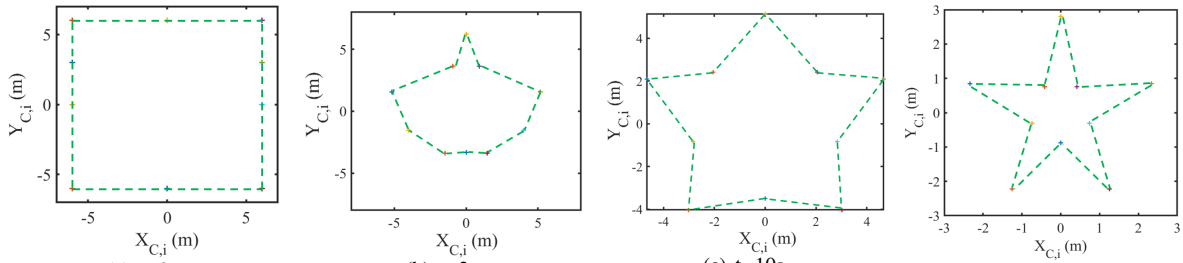

Figure 9: Positions of the 10 agents at t = 0s, 3s, 10s, 20s.

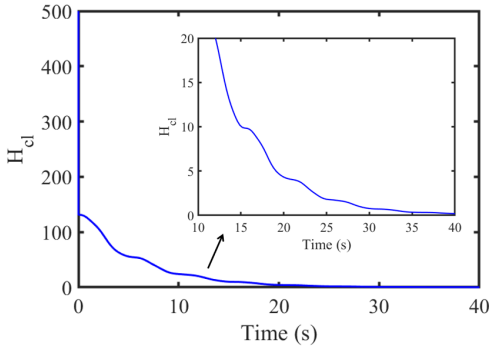

Figure 10: The evolutions of H_{cl} of system (16).

angular momentum p_{i2} are calculated by ([48]),

$$p_{i1} = m_i \sqrt{\dot{X}_{C,i}^2 + \dot{Y}_{C,i}^2}, \quad p_{i2} = I_{cm,i} \frac{\ddot{Y}_{C,i}\dot{X}_{C,i} - \dot{Y}_{C,i}\ddot{X}_{C,i}}{\dot{X}_{C,i}^2 + \dot{Y}_{C,i}^2}. \tag{36}$$

Remark 5. *Since the system trajectory $q_i(t)$ is continuous and remains in a constant state only at the equilibrium, it follows that the denominator of p_{i2} is 0 when and only when the equilibrium is reached. Therefore, before the system reaches the equilibrium, p_{i2} can be solved by using* (36)*. And when the equilibrium is reached, we let $p_{i2} = 0$.*

Furthermore, by virtue of (34) and (36), the heading angle ϕ_i and the equivalent control input u_i are

$$\phi_i(t) = \phi_i(0) + \int_0^t \frac{1}{I_{cm,i}} p_{i2}(t), \quad u_i(t) = \dot{p}_i(t). \tag{37}$$

Remark 6. *We are going to design a controller for the ith PH system to drive the state from $q_i(0)$ to q_i^*, where q_i^* is the equilibrium of* (16)*. According to the specific control objectives, we can design different controllers. For example, the shortest distance is desirable from the perspective of fuel efficiency. Hence, we control the ith agent ($i \in \mathcal{V}$) to run to q_i^* in a straight line from $q_i(0)$. A multitude of related studies have been conducted on the controller design of PH systems with known initial and final positions. Therefore, this paper will not elaborate on this aspect.*

5.2. Simulations of system (25) *(disturbing the PH structure)*

5.2.1. Simulation results

It is easy to find that Assumption 1 is satisfied in the designed value function (35). And the parameters k_1, k_2, γ are chosen properly by (26) in Theorem 4.3. Choosing $v_i(0) = (0, 0)^\top$. By system (25), the evolutions of X_{Ci} and Y_{Ci} are shown in Fig.11 and Fig.12, respectively. Fig.13 illustrates the positions of 10 agents at 0s, 5s, 10s, and 20s.

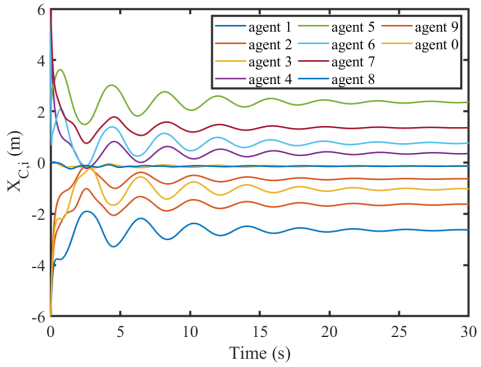

Figure 11: The evolutions of $X_{C,i}$ of system (25).

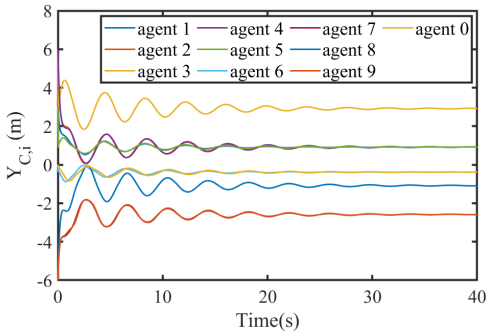

Figure 12: The evolutions of $Y_{C,i}$ in system (25).

Fig.11-Fig.13 shows that the system reached the desired shape. As is shown in Fig.13, when $t = 0$, agents began to move around the square. At 5s, the shape of a pentagram is almost formed, but this is not entirely consistent with the desired shape in the formation objective. Finally, the system stabilized to a predefined pentagram after fine-tuning. The entire motion video can be seen via the link: *https://youtu.be/WUWpVX0Tc6c*.

Fig.14 is a three-dimensional diagram that shows the trajectory changes of x_{Ci} and y_{Ci} over time. The multiple PH systems converge to the pentagram shape (green dotted line) with center $(0, 0)$ from the initial point (red points) under the proposed algorithm, which satisfies the formation objective.

The above simulations illustrate that all wheeled robots move from the square's boundary to its center and are still, after completing the formation of the pentagram shape, realizing the desired formation described in the motivational example. And the actual input u_i can also be calculated by (24).

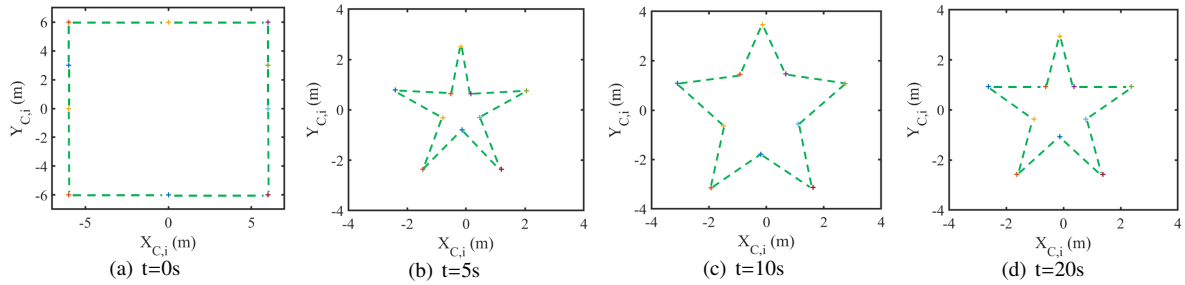

(a) t=0s (b) t=5s (c) t=10s (d) t=20s

Figure 13: Positions of the 10 agents at $t = 0s, 5s, 10s, 20s$.

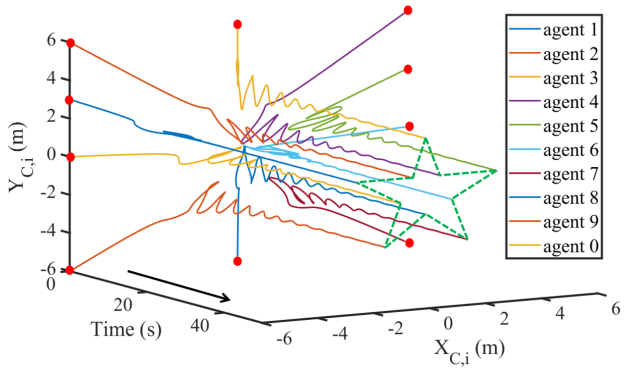

Figure 14: The evolutions of trajectory of system (25).

5.2.2. Parameter analysis

From the proof of Theorem 4.3, we find that the convergence speed of system (25) is not worse than $\zeta = \min\{\frac{\zeta_5}{2}, \frac{\zeta_2-\frac{\zeta_5}{2}}{\varepsilon^3(k_1-\varepsilon)}, \zeta_3, \zeta_6, 2(\zeta_3+\zeta_4-\zeta_5)\}$, then we analyze which parameters have an impact on ζ.

With the definition of ζ_k, $k \in [1{:}6]$, the parameters influencing ζ are: (1) the controller parameters k_1, k_2, γ; (2) the Lyapunov function parameter ε; (3) parameters related to the value function V_i in (9): the strong monotonicity coefficient w and the Lipschitz constant L_g and L_ψ; (4) the number N of agents (5) the smallest positive eigenvalue λ_2 of the Laplacian matrix L of the communication topology.

Obviously, it is difficult to analyze the effects of all parameters simultaneously. Therefore, we only consider selecting some of the parameters for analysis. Since the value function V_i is designed according to the actual requirements of formation control, the weight matrices P_i and Q_i also need to be balanced based on the actual formation goals, we cannot forcibly change them to improve the convergence performance. Therefore, we do not consider the influence of the parameters related to the value function. In addition, the parameter ε is designed for stability analysis, and we cannot use it in the controller so that the influence of ε will not be considered. Hence, only the parameters k_1, k_2, γ, N and λ_2 need to be considered.

It should be noted that the value of k_2 is restricted by constraints in (26). Since the variation range of k_2 is very small, we ignore its influence on the system (25). As the gain of the negative feedback terms in $\dot{v} = -k_1 v - k_2 G(q, \hat{\eta})$ in (25), increasing the value of k_1 will accelerate the convergence speed of the system (25). As shown in Fig.15, the convergence speed of the system trajectory with $k_1 = 20$, $k_2 = 4$ is quicker than that with $k_1 = 8$, $k_2 = 4$. However, we can find that there exists an error between the equilibrium of these two groups of system trajectories. That is because even the value of k_1 is not restricted by a upper bound, if the difference between the selected values of k_1 and k_2 is too large, the system state component v may ignore the influence of $G(q, \hat{\eta})$ and directly converge to 0, which will cause error from the equilibrium of the desired. Therefore, we should not choose an overly large value for k_1. Instead, we need to make a trade-off between the convergence speed and the formation accuracy.

Similarly, as the negative feedback gain of the interaction term $-\gamma(L \otimes I_l)\hat{\eta}$ in (25), increasing the value of γ will also accelerate the convergence speed of the system, enabling the multi-agent systems to quickly achieve a consensus

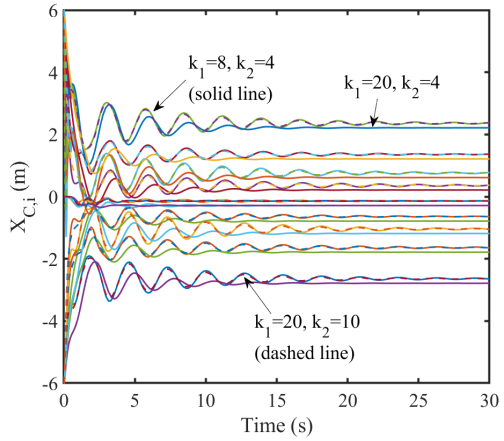

Figure 15: The contrast diagram of the system trajectory $X_{C,i}$ with $k_1 = 8$, $k_2 = 4$ and $k_1 = 20$, $k_2 = 4$.

estimation. The simulation results are shown as Fig.16.

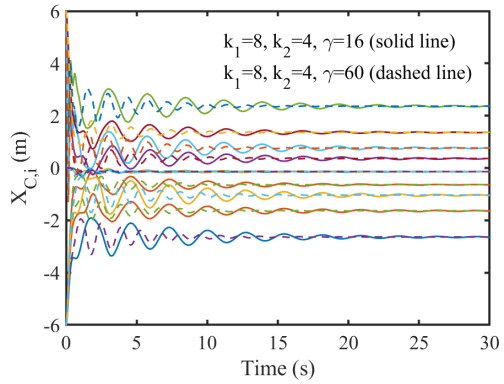

Figure 16: The contrast diagram of the system trajectory $X_{C,i}$ with $\gamma = 16$ and $\gamma = 60$.

Remark 7. *The restriction of inequality* (26) *leads to a very small variation range of* k_2*. However, when* k_2 *does not satisfy the restriction of* (26)*, the system can still converge exponentially to the equilibrium. That is because* (26) *is proposed based on the Lyapunov function chosen in this paper. If we choose another candidate Lyapunov function, the restriction of* k_2 *may be decreased. But as there is currently no theoretical support for the selection of* k_2*, it can only be chosen based on engineering experience or the trial-and-error method. Therefore, the impact of* k_2 *is not analyzed here.*

Next, we will analyze the influence of the agent number N and the eigenvalue λ_2. By recalling the definition of ζ, we have

$$\begin{aligned} &\zeta = \min\{\frac{\zeta_5}{2}, \frac{\zeta_2 - \frac{\zeta_5}{2}}{\varepsilon^3(k_1 - \varepsilon)}, \zeta_3, \zeta_6, 2(\zeta_3 + \zeta_4 - \zeta_5)\}, \\ \text{where}\quad &\zeta_1 = k_1 - \varepsilon - \frac{wk_2}{4\varepsilon} - \frac{k_2 L_f^2}{w\varepsilon} - \frac{5N+4}{4N}L_\psi^2, \quad \zeta_2 = \frac{k_2 w}{2\varepsilon}, \quad \zeta_3 = 1 - \frac{2L_g^2 k_2 \varepsilon}{w}, \\ &\zeta_4 = \gamma\lambda_2 - 8, \quad \zeta_5 = \min\{\zeta_1, \zeta_2\}, \quad \zeta_6 = \min\{\frac{1}{4}, \frac{\zeta_3 + \zeta_4}{2}\}. \end{aligned} \tag{38}$$

By (38), we can find that the increase of N may lead to an increase in k_1, and an increase in λ_2 will only cause an increase in ζ_4, thereby affecting the convergence rate of the system (25). Therefore, if an appropriate communication

topology graph is selected, the convergence speed of the system can be accelerated. Due to the excessive number of selectable graph types, we only present a comparative simulation in Fig.17 to verify our theoretical analysis. Fig.17 shows the contrast diagram of the system trajectory when multi-agent systems communicate with Fig.5 or a fully connected graph (all agents communicate with each other). The convergence speed of system (25) with a fully connected graph $\mathcal{G}_1$ is quicker than they communicating by $\mathcal{G}$ in Fig.5, that is because $\lambda_2(\mathcal{G}_1) = 10 > \lambda_2(G)$.

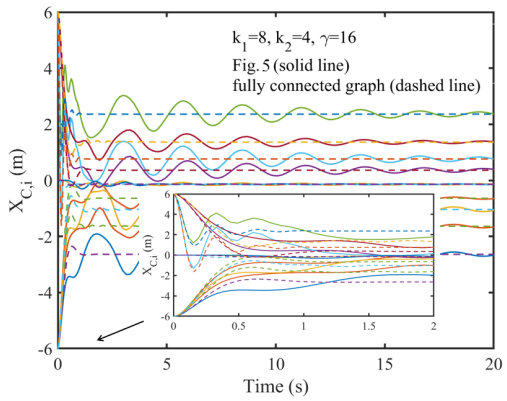

Figure 17: The contrast diagram of the system trajectory $X_{C,i}$ with communication topology as Fig.5 and a fully connected graph.

However, full connectivity requires more channels for information interaction, which poses higher requirements for the communication network. Therefore, we should also balance the communication difficulty and the convergence speed, and select an appropriate communication network to complete the task.

5.3. Comparison of control schemes

With the explanation in the previous subsections, the simulation results demonstrate that the required formation mission of the 10 nonholonomic wheeled robots can be accomplished under the proposed two control methods by designing an appropriate value function. We will then discuss the difference between these two methods.

From the perspective of stability analysis of the closed-loop systems, the first one (16) can maintain the structure of the PH system and has the natural advantage of selecting Hamiltonian as a candidate Lyapunov function, significantly reducing the difficulty of stability analysis. However, this only works when the formation output function satisfies $\psi_i(q_i) = q_i$. The second closed-loop system (25) relaxes the restrictions on $\psi_i(q_i)$ but increases the difficulty of selecting Lyapunov functions in stability analysis. Fortunately, we still found a suitable Lyapunov function to prove the exponential convergence of the system (25) and during the proof process, its minimum convergence rate is given.

A comparison of Fig.7, Fig.8 with Fig.11, Fig.12 reveals that the overshoot is more significantly present in the first closed-loop system (16) than the second one (25). However, this influence may be due to the selection of parameters in the closed-loop system, such as γ, k_1, and k_2. This paper did not provide a theoretical comparison between the two methods and will be considered further in subsequent research.

6. Conclusion

This paper investigates the formation control problem in multi-agent systems with the dynamics described in PH form. After expressing the formation control problem as an optimization objective, two distributed control algorithms with privacy protection are presented, which stabilize the multi-agent systems to the solution of the optimization problem. The first method has the advantage of maintaining the PH closed-loop system structure, which is beneficial for the stability analysis. The second method has quicker convergent speed and smaller overshoot. The efficacy of the proposed approaches is verified through a simulation instance on the pentagram formation control of multiple nonholonomic wheeled robots.

Further work will focus on the trajectory tracking problems of multi-agent systems with time delays and dynamic agent failures. Besides, the communication topology between multi-agent systems may be more complex, such as a directed graph, a time-varying graph, and so on.

Declaration of competing interest

The authors declare that they have no known competing financial interests or personal relationships that could have appeared to influence the work reported in this paper.

References

[1] Hameed A, Ordys A, Możaryn J, Sibilska-Mroziewicz A. Control System Design and Methods for Collaborative Robots: Review. Applied Sciences. 2023;13(1):675.

[2] Zhou Y, Li D, Gao F. Optimal Synchronization Control for Heterogeneous Multi-agent Systems: Online Adaptive Learning Solutions. Asian Journal of Control. 2022;24(5).

[3] Rekabi F, Shirazi F, Sadigh M. Distributed Nonlinear H ∞ Control Algorithm for Multi-Agent Quadrotor Formation Flying. ISA Transactions. 2020;96:81-94.

[4] Du Z, Qu X, Shi J, Lu J. Formation Control of Fixed-Wing UAVs with Communication Delay. ISA Transactions. 2024;146:154-64.

[5] Yu J, Dong X, Li Q, Lu J, Ren Z. Adaptive Practical Optimal Time-Varying Formation Tracking Control for Disturbed High-Order Multi-Agent Systems. IEEE Transactions on Circuits and Systems I: Regular Papers. 2022;69(6):2567-78.

[6] Cai Y, Zhang H, Wang Y, Zhang J, He Q. Fixed-Time Time-Varying Formation Tracking for Nonlinear Multi-Agent Systems under Event-Triggered Mechanism. Information Sciences. 2021;564:45-70.

[7] Li Z, Zhao Y, Yan H, Zhang H, Zeng L, Wang X. Active Disturbance Rejection Formation Tracking Control for Uncertain Nonlinear Multi-Agent Systems With Switching Topology via Dynamic Event-Triggered Extended State Observer. IEEE Transactions on Circuits and Systems I: Regular Papers. 2023;70(1):518-29.

[8] Yue D, Cao J, Li Q, Abdel-Aty M. Distributed Neuro-Adaptive Formation Control for Uncertain Multi-Agent Systems: Node- and Edge-Based Designs. IEEE Transactions on Network Science and Engineering. 2020;7(4):2656-66.

[9] Zhang L, Zheng Y, Huang Z, Huang B, Su Y. Distributed Global Output-Feedback Formation Control without Velocity Measurement for Multiple Unmanned Surface Vehicles. ISA Transactions. 2024;147:118-29.

[10] Goodwine B, Antsaklis P. Multi-Agent Compositional Stability Exploiting System Symmetries. Automatica. 2013;49(11):3158-66.

[11] Deng Z, Luo J, Liu Y, Yu W. Distributed Formation Control Algorithms for QUAVs Based on Aggregative Games. IEEE Systems Journal. 2023;17(3):4419-29.

[12] Deng Z. Game-Based Formation Control of High-Order Multi-Agent Systems. IEEE Transactions on Network Science and Engineering. 2023;10(1):140-51.

[13] Lee D, He N, Kamalaruban P, Cevher V. Optimization for Reinforcement Learning: From a Single Agent to Cooperative Agents. IEEE Signal Processing Magazine. 2020;37(3):123-35.

[14] Van der Schaft A, Jeltsema D. Port-Hamiltonian Systems Theory: An Introductory Overview. Foundations and Trends® in Systems and Control. 2014;1(2):173-378.

[15] Ortega R, van der Schaft A, Maschke B, Mareels I. Putting Energy Back in Control. IEEE Control Systems. 2001;21(2):18-33.

[16] Matei I, Mavridis C, Baras J, Zhenirovskyy M. Inferring Particle Interaction Physical Models and Their Dynamical Properties. In: 2019 IEEE 58th Conference on Decision and Control (CDC). Nice, France: IEEE; 2019. p. 4615-21.

[17] Donaire A, Romero J, Perez T. Trajectory Tracking Passivity-Based Control for Marine Vehicles Subject to Disturbances. Journal of the Franklin Institute. 2017;354(5):2167-82.

[18] Javanmardi N, Yaghmaei A, Yazdanpanah M. Spacecraft Formation Flying in the Port-Hamiltonian Framework. Nonlinear Dynamics. 2020 Mar;99(4):2765-83.

[19] Kumar L, Dhillon S. Tracking Control Design for Fractional Order Systems: A Passivity-Based Port-Hamiltonian Framework. ISA Transactions. 2023;(138):1-9.

[20] Vos E, Van Der Schaft A, Scherpen J. Formation Control and Velocity Tracking for a Group of Nonholonomic Wheeled Robots. IEEE Transactions on Automatic Control. 2016;61(9):2702-7.

[21] Jafarian M, Vos E, De Persis C, Van Der Schaft A, Scherpen J. Formation Control of a Multi-Agent System Subject to Coulomb Friction. Automatica. 2015;61:253-62.

[22] Li N, Borja P, van der Schaft A, Scherpen J. Angle-based formation stabilization and maneuvers in port-Hamiltonian form with bearing and velocity measurements. https://doiorg/1048550/arXiv230509991. 2023.

[23] Li N, Scherpen J, Van Der Schaft A, Sun Z. A Passivity Approach in Port-Hamiltonian Form for Formation Control and Velocity Tracking. In: 2022 European Control Conference (ECC). London, United Kingdom: IEEE; 2022. p. 1844-9.

[24] Liang C, Ge M, Xu J, Liu Z, Liu F. Secure and Privacy-Preserving Formation Control for Networked Marine Surface Vehicles With Sampled-Data Interactions. IEEE Transactions on Vehicular Technology. 2022;71(2):1307-18.

[25] Yue J, Qin K, Shi M, Jiang B, Li W, Shi L. Event-Trigger-Based Finite-Time Privacy-Preserving Formation Control for Multi-UAV System. Drones. 2023;7(4):235.

[26] Acar A, Aksu H, Uluagac A, Conti M. A Survey on Homomorphic Encryption Schemes: Theory and Implementation. ACM computing surveys. 2018;51(4):1-35.

[27] Li N, Lyu M, Su D, Yang W. Differential Privacy: From Theory to Practice. Synthesis Lectures on Information Security, Privacy, and Trust. Cham: Springer International Publishing; 2017.

[28] Kang S, Ahn H. Design and Realization of Distributed Adaptive Formation Control Law for Multi-Agent Systems With Moving Leader. IEEE Transactions on Industrial Electronics. 2016;63(2):1268-79.

[29] Li Y, Wu Y, He S. Network-Based Leader-Following Formation Control of Second-Order Autonomous Unmanned Systems. Journal of the Franklin Institute. 2021;358(1):757-75.

[30] Li N, Sun Z, van der Schaft A, Scherpen J. A Port-Hamiltonian Framework for Displacement-Based and Rigid Formation Tracking, https://doi.org/10.48550/arXiv.2305.09964.; 2023.
[31] Tao H, Guan Z, Chi M, Hu B, Li Z. Multi-Formation Control of Nonlinear Leader-Following Multi-Agent Systems. ISA Transactions. 2017;69:140-7.
[32] Jafarian M, Vos E, De Persis C, Scherpen J, van der Schaft A. Disturbance Rejection in Formation Keeping Control of Nonholonomic Wheeled Robots. International Journal of Robust and Nonlinear Control. 2016;26(15):3344-62.
[33] Li H, Wang C, Yin Z, Xi J, Zheng Y. Optimal Distributed Time-Varying Formation Control for Second-Order Multiagent Systems: LQR-based Method. ISA Transactions. 2024;152:177-90.
[34] Fabiani F, Fenucci D, Fabbri T, Caiti A. A Passivity-Based Framework for Coordinated Distributed Control of AUV Teams: Guaranteeing Stability in Presence of Range Communication Constraints. In: OCEANS 2016 MTS/IEEE Monterey. Monterey, CA, USA: IEEE; 2016. p. 1-5.
[35] El-Ferik S, Qureshi A, Lewis F. Robust Neuro-Adaptive Cooperative Control of Multi-Agent Port-Controlled Hamiltonian Systems. International Journal of Adaptive Control and Signal Processing. 2016;30(3):488-510.
[36] Gould R. Graph Theory. Menlo Park, Calif.: Benjamin/Cummings Pub. Co.; 1988.
[37] Mordukhovich B. Variational Analysis and Applications. Springer Monographs in Mathematics. Cham: Springer International Publishing; 2018.
[38] Yang Y, Xiao Y, Li T. A Survey of Autonomous Underwater Vehicle Formation: Performance, Formation Control, and Communication Capability. IEEE Communications Surveys & Tutorials. 2021;23(2):815-41.
[39] Das A, Fierro R, Kumar V, Ostrowski J, Spletzer J, Taylor C. A Vision-Based Formation Control Framework. IEEE Transactions on Robotics and Automation. 2002;18(5):813-25.
[40] Dong X, Hu G. Time-Varying Formation Control for General Linear Multi-Agent Systems with Switching Directed Topologies. Automatica. 2016;73:47-55.
[41] Feng S, Kawano Y, Cucuzzella M, Scherpen J. Output Consensus Control for Linear Port-Hamiltonian Systems. IFAC-PapersOnLine. 2022;55(30):230-5.
[42] Lv J, Chen F, Chen G. Nonsmooth Leader-Following Formation Control of Nonidentical Multi-Agent Systems with Directed Communication Topologies. Automatica. 2016;64:112-20.
[43] Tang Y, Zhang D, Shi P, Zhang W, Qian F. Event-Based Formation Control for Nonlinear Multiagent Systems Under DoS Attacks. IEEE Transactions on Automatic Control. 2021;66(1):452-9.
[44] Cao Y, Yu W, Ren W, Chen G. An Overview of Recent Progress in the Study of Distributed Multi-Agent Coordination. IEEE Transactions on Industrial Informatics. 2013;9(1):427-38.
[45] Lin W, Li C, Qu Z, Simaan M. Distributed Formation Control with Open-Loop Nash Strategy. Automatica. 2019;106:266-73.
[46] Zhang C, Wang Y. Enabling Privacy-Preservation in Decentralized Optimization. IEEE Transactions on Control of Network Systems. 2019;6(2):679-89.
[47] Facchinei F, Kanzow C. Generalized Nash Equilibrium Problems. Annals of Operations Research. 2010;175(1):177-211.
[48] Wei J, Zhu B. Model Predictive Control for Trajectory-Tracking and Formation of Wheeled Mobile Robots. Neural Computing and Applications. 2022;34(19):16351-65.